11. UPPER IMBRIAN SERIES

FIGURE 11.1 (OVERLEAF).—Region centered on Apollo 11 landing site in Mare Tranquillitatis (arrow). Large crater at bottom is Theophilus (100 km). Rings of Procellarum basin pass under mare-ridge feature Lamont (ring and radial pattern above arrow) and through rugged terra at right. Telescopic photograph by the Pic du Midi Observatory, France.

11. UPPER IMBRIAN SERIES

CONTENTS

INTRODUCTION

The Upper Imbrian Series contains extensive mare materials, subordinate crater materials, and no basins at all (pl. 9; fig. 11.1). This geologic style contrasts sharply with the exposed record of the earlier, impact-dominated era (see chaps. 8–10; pls. 6–8), which ended with the Orientale impact. Only on the farside and only if exterior deposits are considered (as shown for craters larger than 60 km in diameter on pl. 9) do Upper Imbrian crater deposits exceed Upper Imbrian maria in area.

Two-thirds of the nearside mare surface is Upper Imbrian. Because of this extent and because the Imbrium impact struck the nearside, beginning the Imbrian Period, the Imbrian System dominates the nearside (pls. 8, 9). Absence of an Imbrian cover leaves the pre-Nectarian and Nectarian impact materials, which doubtless formed randomly on the whole Moon, as the dominant deposits on the farside (pls. 6, 7).

Upper Imbrian mare units furnished more samples than any other class of lunar geologic unit, because of their accessibility to landings and their prominence on the nearside. Samples of mare basalt were returned from all landing sites (see chap. 5; table 1.2), and seven of these sites furnished data on absolute ages and composition that are useful in regional studies like the present one. Only one of these seven sampling missions, Apollo 12, returned basalt that is here regarded as younger than Imbrian (see chap. 12).

The emphasis in this chapter corresponds to the relative importance of the two main types of lunar materials in the Upper Imbrian Series. Craters are described briefly in the first section after the series definition. The rest of the chapter describes the general stratigraphy of each major mare or mare cluster and describes in detail the absolute ages and stratigraphy for those maria from which basaltic samples were collected. I show that the volume, sequence, and composition of basaltic eruptions were fundamentally predetermined in the foregoing era, when basin impacts thinned the crust, uplifted the mantle, and weakened the lithosphere.

DEFINITION

The bottom of the Upper Imbrian Series is the top of the Orientale-basin deposits (see chap. 10). Frequencies of 2.2×10^{-2} craters at least 1 km in diameter per square kilometer and D_L values of 550 m,

therefore, are approximate maximums for the Upper Imbrian Series (figs. 10.37, 11.2; tables 7.3, 11.1). To my knowledge, the largest frequencies actually determined on Upper Imbrian materials are about 2×10^{-2} craters of this size per square kilometer, for old, probably unsampled units near the Apollo 11 landing site (Neukum and others, 1975b; compiled from data of Greeley and Gault, 1970). The large error bar for this determination (table 11.1) overlaps the crater frequency for the older Orientale basin and demonstrates the imprecision of such counts for small mare units. The largest D_L value measured on a mare unit is 390 m, for a spot in Mare Nectaris (Boyce and others, 1975).

No stratigraphic unit comparable to the Orientale deposits defines the top of the Upper Imbrian Series and the Imbrian System, because the individual mare and crater units that formed after Orientale do not cover a sufficient area to be globally useful as stratigraphic-datum horizons. Therefore, the boundary is defined on the basis of D_L values.

TABLE 11.1.—*Properties of the Upper Imbrian Series and adjacent time-stratigraphic units*

[References: B75, Boyce and others (1975); B76, Boyce (1976); M80b, Moore and others (1980b); N75a, Neukum and others (1975a); N75b, Neukum and others (1975b); SL72, Soderblom and Lebofsky (1972). Crater frequencies: Cumulative, determined by normalization, using a calibration curve and commonly based on craters smaller than 1 km in diameter (see fig. 7.10G; Neukum and others, 1975b). Ages: Radiometric ages obtained from samples collected from the listed rock-stratigraphic units (see tables 10.1, 11.3, 12.4)]

Time-stratigraphic unit	Rock-stratigraphic unit: Mare group	Rock-stratigraphic unit: Formation	Crater frequency (larger than 1 km in diameter per square kilometer)	Reference	D_L (m)	Reference	Age (aeons)
Eratosthenian System.	---	Apollo 12 mare----	$2.4^{+0.3}_{-0.4} \times 10^{-3}$	N75b	210±20 210±30 215±45	B76 SL72 SL72	3.16
Upper Imbrian Series.	3	Apollo 15 mare----	$2.6^{+0.6}_{-0.4} \times 10^{-3}$	N75a, N75b	270±15	B76	3.25
	3	Eastern Mare Crisium.	Approx 2.6×10^{-3}	N75a	----------		
	3	Central Mare Serenitatis.	3.9×10^{-3}	N75a	225-320	B75	---
	3	Luna 16 mare----------			270±30	B76	3.40
	2	Apollo 11 mare----	$3.4^{+3.6}_{-1.6} \times 10^{-3}$	N75b	320±40 330±40 335±55	SL72 SL72 B76	3.57
	2	Apollo 17 mare----	$9.0^{+2.3}_{-3.0} \times 10^{-3}$	N75b	360±30 365±30	B76 M80b	3.72
	2	Old flows near the Apollo 11 landing site.	$2.0^{+2.0}_{-1.0} \times 10^{-2}$	N75b	----------		
Lower Imbrian Series.	---	Orientale basin---	2.2×10^{-2}	N75a, N75b	550±50	Chapter 10	---
	---	Imbrium basin-----	$2.5\text{-}4.8 \times 10^{-2}$	N75a, N75b	----------		3.85

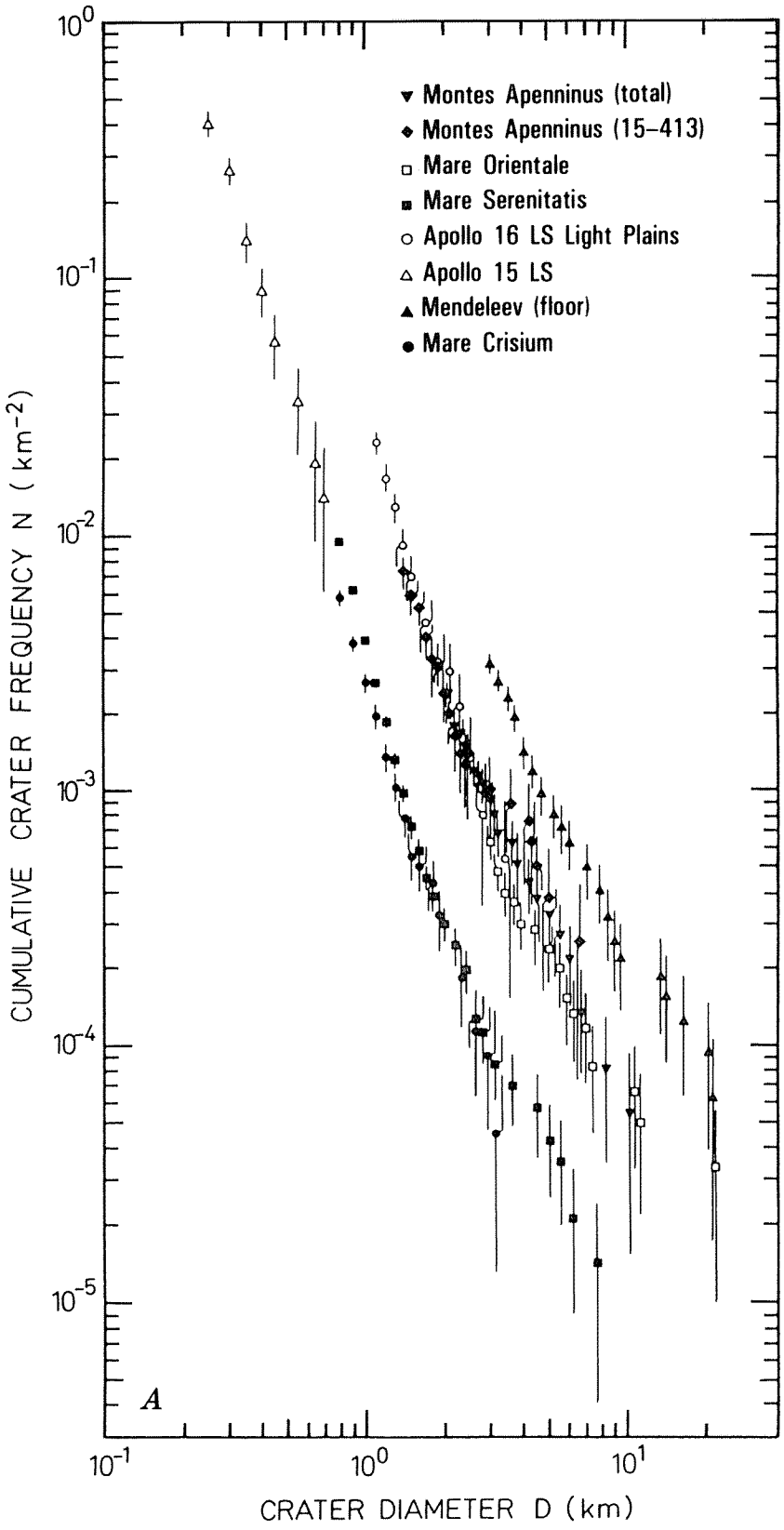

FIGURE 11.2.—Crater frequencies of units of Upper Imbrian and other ages.

A. Distinct curves for three time-stratigraphic units: (1) Nectarian System—plains on floor of Mendeleev; (2) Lower Imbrian Series—Montes Apenninus flank (two curves), light plains at Apollo 16 landing site (LS), and "Mare Orientale," actually Orientale basin (compare fig. 10.37); (3) Upper Imbrian Series—eastern Mare Crisium, Palus Putredinis near Apollo 15 landing site (both sides of Rima Hadley), and two-thirds of central Mare Serenitatis. Upper Imbrian units are near upper boundary of the series. From Neukum and others (1975a, fig. 6).

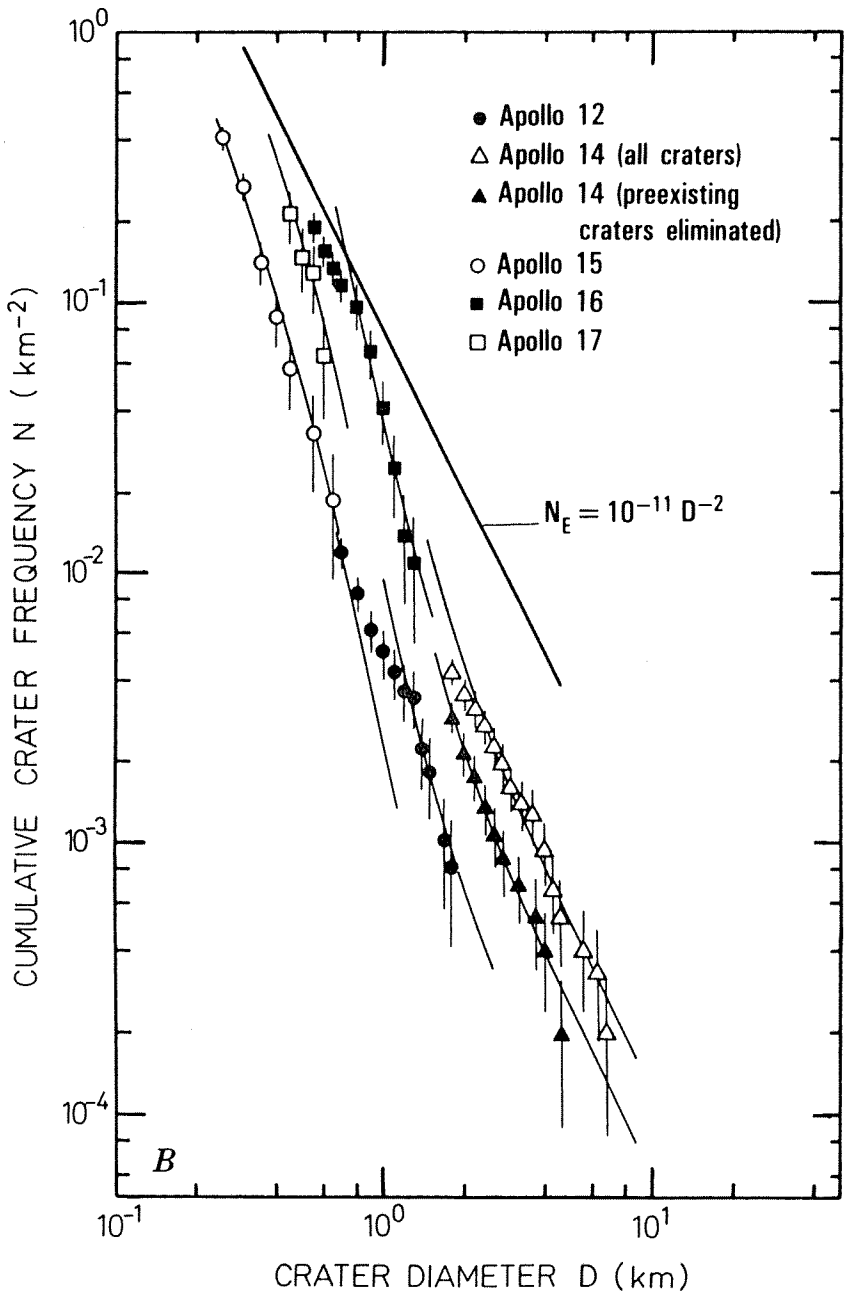

B. Upper Imbrian Apollo 15 mare in comparison with older and younger units. Apollo 17 mare (sparse data) is also Upper Imbrian. Offset in Apollo 12 curve shows that data for two units are combined—an older Upper Imbrian unit not sampled and an Eratosthenian unit that probably was sampled (see chap. 12); Eratosthenian unit is barely younger than Apollo 15 mare. Lower Imbrian units (see chap. 10) are Apollo 16 Cayley plains and Fra Mauro Formation in area of Apollo 14 landing site; one Apollo 14 count ("all craters") is hybrid of superposed and buried craters. Curve N_E is equilibrium (steady state) curve of Trask (1966); Apollo 16 plot shows rollover near steady state at about 800-m crater diameter (table 7.4); craters too small to count would show rollover for younger units. From Neukum and others (1975b, fig. 7).

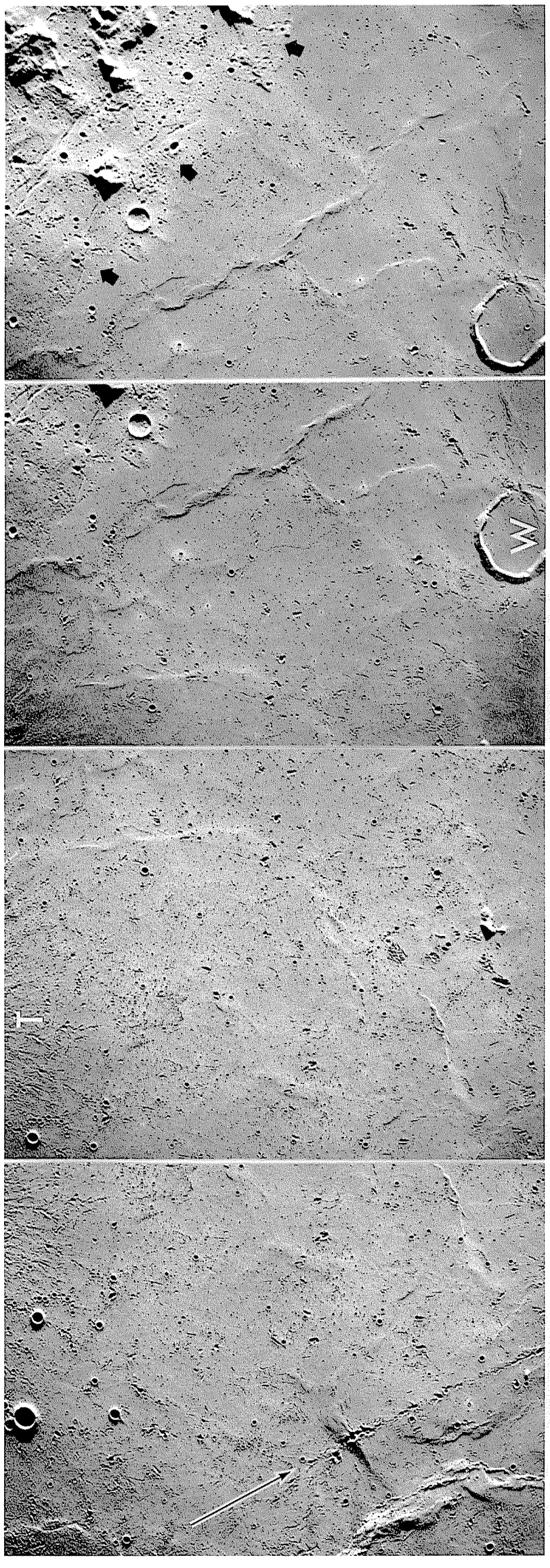

FIGURE 11.3.—Type area of top of Imbrian System. Most of area is covered by mare material older than superposed secondary craters of Eratosthenes (centered 250 km south in direction of arrow) and of Timocharis (T, fan-shaped pattern). D_L values average 270 m (Boyce, 1976); subunits are indistinct because of secondaries. Patches in, north of, and east of Wallace (W; 26 km) are probably Eratosthenian; patch north of (above) Wallace has $D_L = 220 \pm 30$ m (Boyce and others, 1975). Mare truncates Lower Imbrian Apennine Bench Formation and secondary craters of Archimedes superposed thereon (black arrows; compare fig. 10.1). Stereoscopic overlap of Apollo 17 frames M–2114, M–2115, M–2117, and M–2119 (from right to left).

Boyce and others (1975) determined that the mare units between Eratosthenes and Archimedes (figs. 1.6, 2.1, 10.1, 11.3) have D_L values from 190 to 340 m, including error ranges; midpoints range from 220 to 290 m. Wilhelms (1980) observed that units here and in the rest of southern Mare Imbrium which have D_L values less than 230 m match Eratosthenian units as traditionally mapped, and that units with D_L values greater than 250 m match Imbrian units. Therefore, he proposed these values as working criteria for the Imbrian-Eratosthenian boundary. Units with D_L values from 230 to 250 m were to be assigned on the weight of other evidence. This definition, though not formally rigorous, has served conveniently to divide a maximum number of units into Imbrian and Eratosthenian age groups that harmonize with existing mapping. This working criterion of $D_L = 240 \pm 10$ m for the upper boundary of the Imbrian System and of the Upper Imbrian Series is used here.

The characteristic size-frequency distribution for the upper boundary of the system and the series is less well defined than those for Imbrium- and Orientale-basin deposits because of the statistical unreliability of counts for the small units typical of maria. The similar values determined by Neukum and others (1975a, b) for central Mare Serenitatis, the region of the Apollo 15 landing site, and eastern Mare Crisium are probably representative of units near the upper boundary (fig. 11.2; table 11.1). Midpoints of these determinations range about from 2.6×10^{-3} to 3.9×10^{-3} craters at least 1 km in diameter per square kilometer.

Thus, the total range of observed Upper Imbrian cumulative frequencies of such craters per square kilometer is from about 2.2×10^{-2} for the Orientale basin to 2.6×10^{-3} for these young mare units (figs. 10.4, 11.2; tables 7.3, 11.1). Figures 7.15 and 12.8 and tables 7.3 and 11.1 give some equivalent D_L and crater-frequency values. As discussed in chapters 12 and 13, the values on terra-breccia and mare-basalt units are not directly comparable. Interpolations between values for breccia deposits and mare lavas are hazardous because the correction factor for the Imbrian System has not yet been determined. Thus, some of the units considered here to be Upper Imbrian may be Eratosthenian, and vice versa.

CRATER MATERIALS

Recognition criteria

Some large craters can readily be assigned to the Upper Imbrian Series by stratigraphic criteria (table 11.2). An example is Schlüter, which is superposed on Orientale deposits but slightly flooded by mare material (fig. 11.4).

TABLE 11.2.—*Representative Upper Imbrian craters*

[Cross rules divide diameter ranges mapped differently in plate 9: smaller than 30 km, unmapped; 30 to 59 km, interiors mapped; 60 km and larger, exterior deposits mapped where exposed. E?, possibly Eratosthenian; LI?, possibly Lower Imbrian]

Crater	Diameter (km)	Center (lat)	Center (long)	Figure	Remarks
St. George-----	2.3	25.9° N.	3.4° E.	5.11	Apollo 15.
Bonpland D-----	6	10° S.	18° W.	6.6	Faulted.
Ariadaeus B----	8	5° N.	15° E.	10.38	Typical.
Lansberg C-----	17	2° S.	29° W.	10.41	Flooded.
Daedalus S-----	20	7° S.	173° E.	8.7	LI?
Krieger--------	22	29° N.	46° W.	11.6	Asymmetric (see table 7.2).
Vitruvius------	30	18° N.	31° E.	9.13	LI?
Timaeus--------	33	63° N.	0.5° W.	10.15	---
Bianchini------	38	49° N.	34° W.	3.8	---
Lansberg-------	39	0°	27° W.	10.41, 13.10	LI?
Mairan---------	40	42° N.	43° W.	3.8	---
Sharp----------	40	46° N.	40° W.	3.8	E?
Stiborius------	44	34° S.	32° E.	11.5, 11.7	---
Cardanus-------	50	13° N.	72° W.	10.3, 11.8	Typical.
Krafft---------	51	17° N.	73° W.	10.3, 11.8	Twin of Cardanus.
Lindenau-------	53	32° S.	25° E.	11.5	---
Thebit---------	57	22° S.	4° W.	7.7	---
Jenner---------	72	42° S.	96° E.	1.3, 1.5, 10.46	Sandwiched by mare units.
Archimedes-----	83	30° N.	4° W.	1.6, 6.10, 10.1	Mare fill.
Atlas----------	87	47° N.	44° E.	1.7, 9.3	Floor uplifted.
Piccolomini----	88	30° S.	32° E.	11.7	LI?
Schlüter-------	89	6° S.	83° W.	11.4	Typical.
Posidonius-----	95	32° N.	30° E.	1.7, 5.17, 2.5D	LI?; floor uplifted.
Plato----------	101	52° N.	9° W.	1.6, 7.3	Mare fill.
Antoniadi------	135	70° S.	172° W.	1.5, 4.2A	LI?; interior ring.
Tsiolkovskiy---	180	20° S.	129° E.	1.3, 1.4, 3.24, 3.27	Mare fill.
Humboldt-------	207	27° S.	81° E.	1.5, 4.2E, 9.6, 10.46	Floor uplifted.
Iridum---------	260	44° N.	31° W.	1.6, 3.8, 10.43	Half-buried.

Other crater materials can be compared with the well-dated ones by means of crater densities where photographs are adequate and where exposed surfaces are large enough to underlie a statistically valid number of craters. These conditions are rarely met for craters of the Imbrian System. D.B. Snyder (written commun., 1980) determined that the Iridum crater (fig. 3.8) is Upper Imbrian and that Petavius (table 10.2) is Lower Imbrian. Most crater units, however, are too small or too poorly photographed to permit counts of a statistically significant number of superposed craters larger than the steady-state diameters (approx 300–800 m for the Imbrian System; see table 7.3).

Qualitative estimates of the age significance of erosional morphology are, therefore, used here more than stratigraphic or size-frequency criteria to determine the ages of craters larger than 2 or 3 km in diameter within the Imbrian System. Morphology reflects erosion by small impacts, many of whose individual craters are now obliterated because they are in a steady state. The radial ejecta and secondary-crater groups of many large craters considered to be Late Imbrian are conspicuous, though slightly blurred and visibly cratered; examples are Tsiolkovskiy (figs. 3.24, 3.27; Guest and Murray, 1969) and Lindenau (fig. 11.5). Krieger, embayed by Late Imbrian mare materials, is a very fresh Late Imbrian crater (fig. 11.6). In general, however, assignments to the Lower or Upper Imbrian Series are less secure than those to a system. For example, such outlying craters as Piccolomini that are more subdued than Eratosthenian craters and are superposed on Imbrium-basin secondaries must be Imbrian (fig. 11.7), but whether they are Lower or Upper Imbrian is less clear.

Frequency

Plate 9 shows a total of 162 unburied Upper Imbrian craters larger than 30 km in diameter within an area of 35.3×10^6 km^2 that excludes younger deposits from the total lunar area of 38×10^6 km^2. Extrapolation of this density (4.6 craters per million square kilometers) suggests that 174 such craters formed over the whole Moon during the Late Imbrian Epoch. These values are similar to those for the Lower Imbrian Series (5.1 such craters per million square kilometers or 195 such craters on the whole Moon; see chap. 10). As shown at the end of this chapter, however, the formation rates differed greatly because the two epochs were of unequal duration. The cumulative frequency of Lower and Upper Imbrian craters at least 5 km in diameter superposed on deposits of Imbrium, Orientale, and the Iridum crater—thus, of different maximum ages—is 10^{-4} per square kilometer (figs. 7.16, 10.4; Wilhelms and others, 1978).

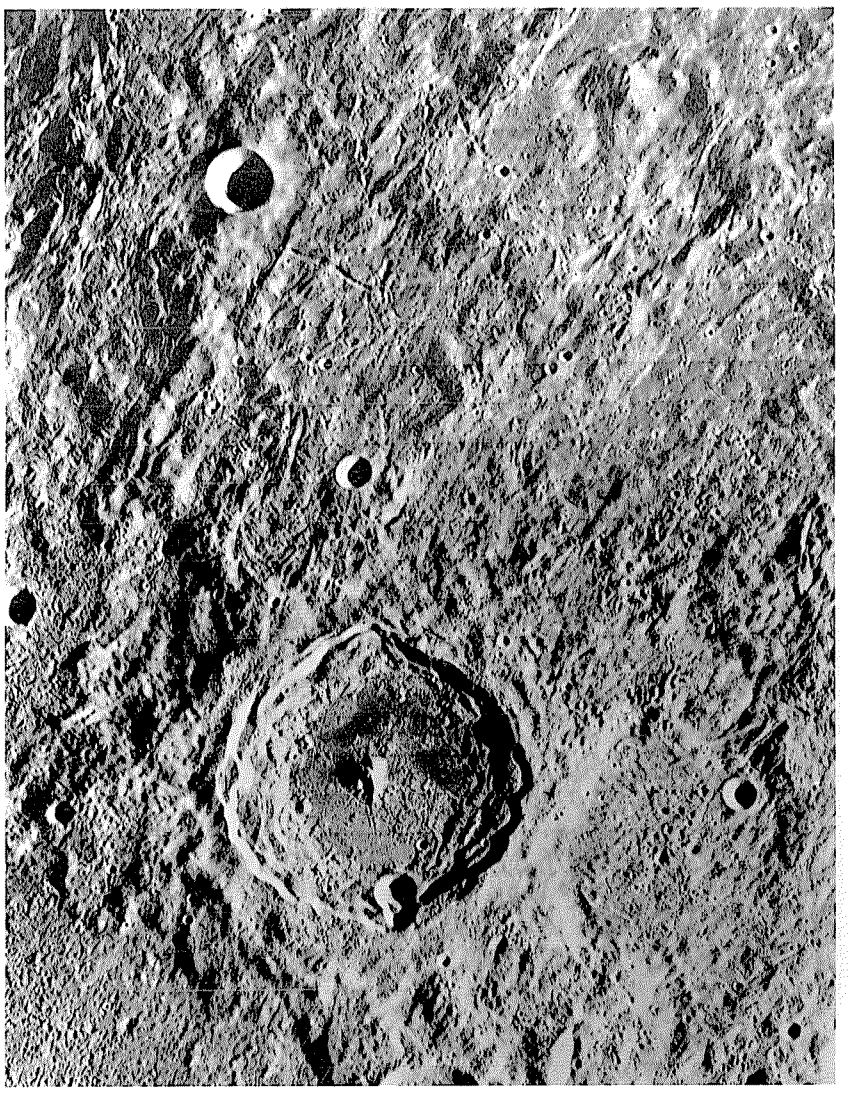

FIGURE 11.4.—Crater Schlüter (89 km, 6° S., 83° W.), superposed on Hevelius Formation at Montes Cordillera (scarp below and left of Schlüter; compare fig. 4.4). Late Imbrian age of Schlüter is indicated by its stratigraphic position between the Hevelius Formation and mare basalt; thus, the morphology and density of small superposed craters are useful for comparison with other areas (fig. 11.5). Orbiter 4 frame H–181.

MARE MATERIALS—GENERAL STRATIGRAPHY AND DISTRIBUTION

Imbrian mare materials are divided here (pl. 9; figs. 11.8, 11.9) into three groups: old (unit 1), intermediate-age (unit 2), and young (unit 3). Finer subdivision is possible in well-photographed areas but not in all maria.

Exposures of the old units are the least extensive; they cover only 0.24×10^6 km^2. They occupy elevated terra tracts in the outer Procellarum-basin shelf and outside this giant pre-Nectarian basin, places where their elevation or presence in a generally mare-poor area protected them from later inundation (figs. 10.3, 10.46, 11.8). They undoubtedly extend beneath the younger units but their extent is unknown. The western Procellarum remnants of the old group are spectrally blue, as are those on the east shelf of Mare Nubium (not distinguished on pl. 4). The more extensive exposures inside and near Oceanus Procellarum in the northeast quadrant of the nearside are spectrally red. Some units of the old group were discussed in chapter 10 because they may be Lower Imbrian (fig. 10.46); however, they are mapped here with other Upper Imbrian units because that is their

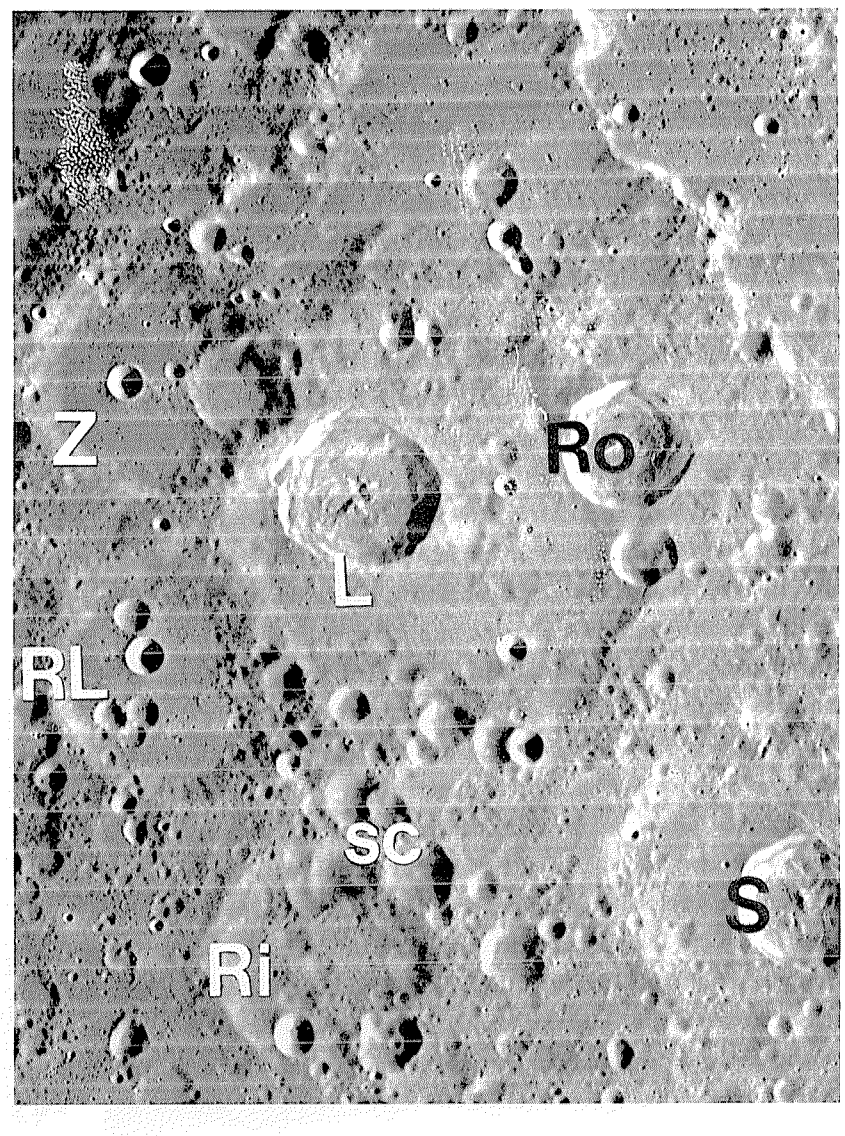

FIGURE 11.5.—Craters Lindenau (L; 53 km, 32° S., 25° E.) and Stiborius (S; 44 km, 34 S., 32 E.), probably Late Imbrian, judging by their similarity to Schlüter (fig. 11.4). Rothmann (Ro; 42 km, 31° S., 28° E.), generally similar though less cratered and slightly sharper despite its smaller size than Lindenau, is probably Eratosthenian. Pre-Nectarian craters buried by Nectaris ejecta include Zagut (Z; 84 km), Rabbi Levi (RL; 81 km), and Riccius (Ri; 71 km); sc, Imbrium-secondary craters superposed on Nectaris ejecta. Orbiter 4 frame H–83.

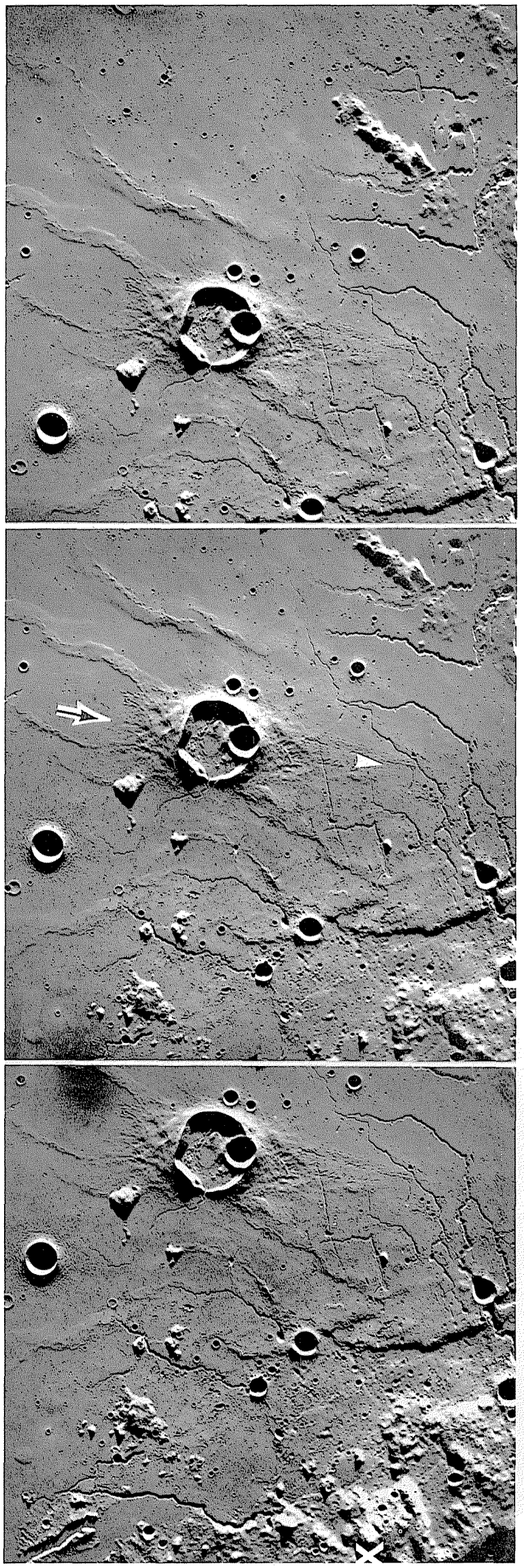

FIGURE 11.6.—Morphologically fresh crater Krieger (22 km, 29° N., 46° W.), both superposed on mare (white arrowhead) and flooded by other mare materials (black-on-white arrow). Crater's freshness suggests an Eratosthenian age, but superpositional relations and number of superposed smaller craters indicate an Imbrian age. Possible Orientale-secondary craters are embayed by dark-mantling materials (X, left). Parts of sinuous-rille systems of the Aristarchus Plateau (left) and Montes Harbinger (lower right) are visible (compare fig. 5.12). Stereoscopic pairs of Apollo 15 frames M–2082, M–2083, and M–2084 (from right to left).

more likely age. D_L values of the old group are larger than 390 m, values that correspond to ages of 3.75 to 3.80 aeons (Boyce, 1976). Size-frequency counts are unavailable.

The intermediate-age and young groups occupy much more area, about 1.19×10^6 and 2.67×10^6 km^2, respectively (pl. 9). D_L values range from 290 to 390 m for the intermediate group and from 240 to 290 m for the young group. These values correpond to ages of 3.50 to 3.75 and 3.20 to 3.50 aeons, respectively (Boyce, 1976). Crater frequencies do not accurately discriminate these groups because the individual units are not sufficiently extensive for statistically valid counting of craters. Table 11.1 lists some typical frequencies for craters at least 1 km in diameter (Neukum and others, 1975a, b). An approximate dividing frequency is 3×10^{-3} such craters per square kilometer, but this value is not intended to be definitive for group assignment. Both groups occur in all nearside maria, although one group may not occupy enough area to be shown on plate 9. The intermediate-age group is abundant in Maria Fecunditatis, Nectaris, Australe, and other maria outside Procellarum, and on shelves and other elevated terrain of many maria. The young group dominates the surfaces of most maria. The intermediate-age and young groups are subequal in Mare Tranquillitatis. On the farside, photographic quality permits subbivision of mare units (Wilbur, 1978; Walker and El-Baz, 1982) only where they are covered by Lunar Orbiter H-frames (parts of Maria Australe and Orientale and in the crater Tsiolkovskiy) or by Apollo orbital photographs (most of the area north of lat 30° S. and west of long 180°; see pl. 2).

The original extent of the three groups is difficult to estimate. Assuming that Imbrian mare units underlie all exposed Eratosthenian and Copernican mare units and all the crater deposits that are superposed on maria (pls. 4, 10, 11), the total area of Imbrian mare units is 6.17×10^6 km^2. If each group covers buried terrain in proportion to its exposure, the total unburied and buried extent of each is: old group, 6.17×10^6 km^2; intermediate-age group, 5.18×10^6 km^2; and young group, 4.01×10^6 km^2. These calculations probably are reasonably accurate for the young group but less accurate for the intermediate-age group and quite uncertain for the old group, which may not have been extruded everywhere that maria are now exposed.

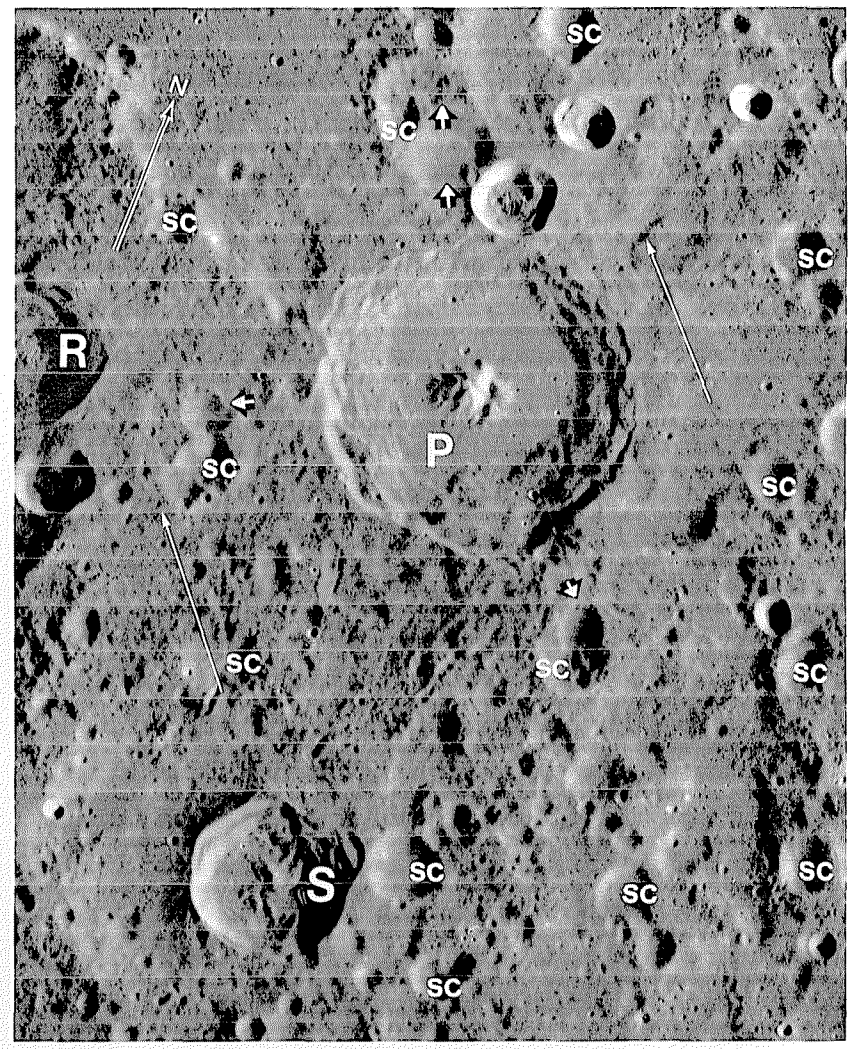

FIGURE 11.7—Crater Piccolomini (P; 88 km, 30° S., 32° E.), superposed on Rupes Altai (under north arrow). Piccolomini deposits are superposed on Imbrium-secondary craters (sc), as indicated by white-on-black arrows. Imbrium-basin rim (Montes Apenninus) is 1,800 km away in direction of white arrows. Craters Rothmann (R) and Stiborius (S) are also visible in figure 11.5. Orbiter 4 frame H–76.

Dark materials that mantle terra topography are also Late Imbrian, judging from the absence of Orientale effects on their surfaces (figs. 5.12, 5.15–5.17, 6.2, 11.6). Most known dark-mantling materials occur along the margins of maria, especially those near the center of the Procellarum basin (pl. 4). Carr (1965b; 1966a, b) observed superpositions of some dark-mantling deposits on mare surfaces (figs. 5.16–5.18) and, accordingly, surmised a volcanic origin (see chap. 5) and an Imbrian or Eratosthenian age. The smoothness and low crater densities of the deposit of dark mantle at the Apollo 17 landing site led later workers to conclude a Copernican age (Scott and Pohn, 1972; Scott and others, 1972; Greeley and Gault, 1973). Embayment relations in several areas showed impingement by mare material on dark-mantled hills (fig. 6.2*B*; Scott and others, 1972), but this evidence was not accepted as definitive of an old age. Subsequent

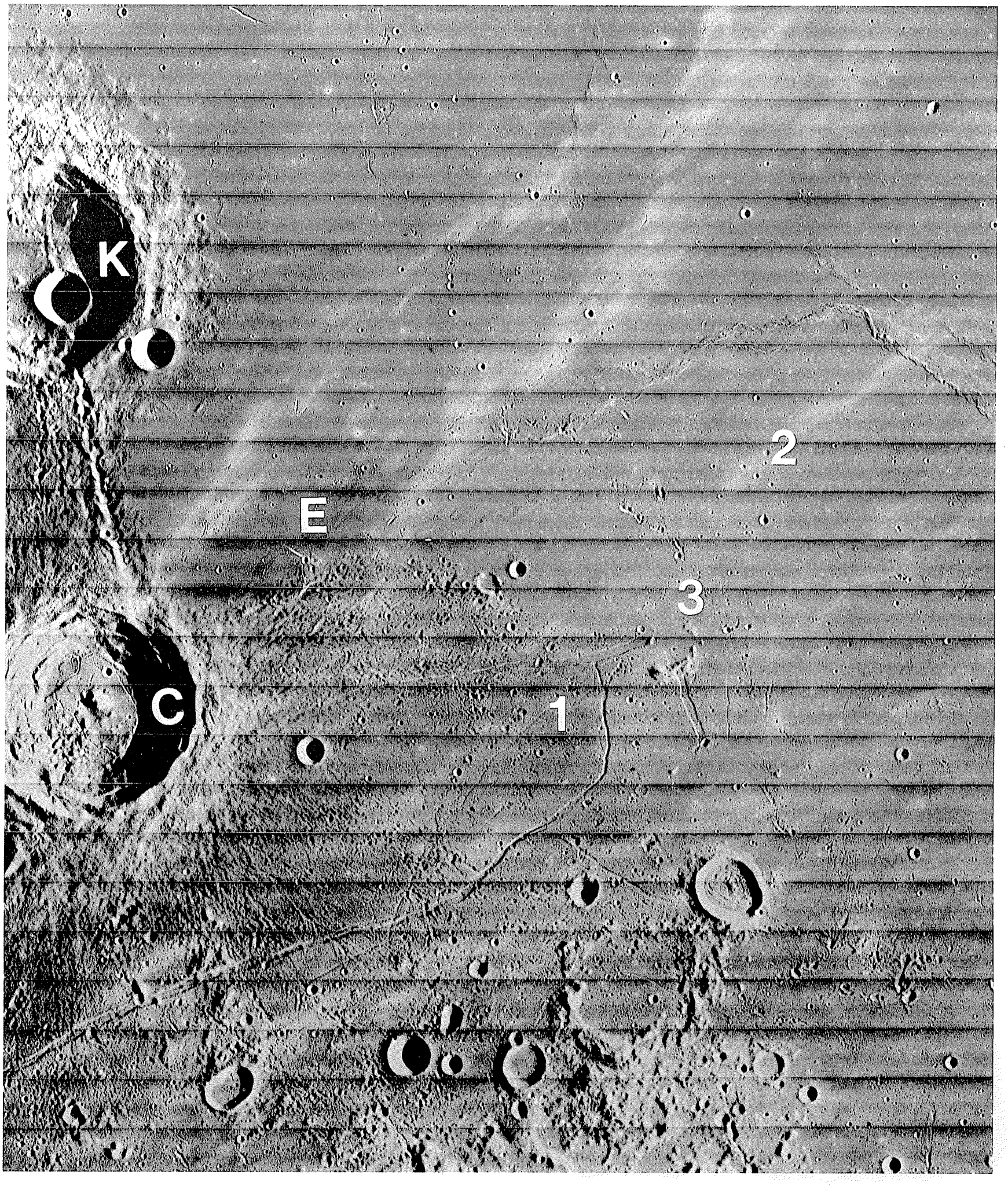

FIGURE 11.8.—Three mare units near craters Krafft (K; 51 km, 17° N., 73° W.) and Cardanus (C; 50 km, 13° N., 72° W.; compare fig. 10.3). Old unit (1) underlying Cardanus ejecta is sharply truncated by units of uppermost Upper Imbrian group (3) and Eratosthenian System (E; pl. 10). Patches too small to show on plate 9 may belong to middle Upper Imbrian group (2). Orbiter 4 frame H–169.

results, however, have confirmed the validity of the photogeologic observations of embayments; post-Imbrian dark-mantling deposits are rare.

The following six sections describe the sampled Upper Imbrian maria in order of decreasing absolute age of their oldest samples. The Apollo 11 suite contains basalt of both the old and intermediate-age Late Imbrian groups, as well as some Early Imbrian basalt. The next two suites, from the Apollo 16 (one fragment) and Apollo 17 landing sites, fall entirely within the intermediate-age group. The last three Imbrian suites are in the young group. The rest of this chapter discusses unsampled maria according to their position relative to the Procellarum basin, which, I believe, has controlled mare distribution (pls. 4, 9–11) by thinning the elastic lithosphere and terra crust as a prelude to the additional thinning inflicted by the immediate mare host basins.

MARE TRANQUILLITATIS

General stratigraphy

Mare Tranquillitatis occupies a pre-Nectarian basin, about 800 km in diameter, with irregular margins and without definite multiple-ring structure (fig. 11.1). The irregular topography in and near this basin results from the intersection of the Tranquillitatis, Nectaris, Crisium, Fecunditatis, and Serenitatis basins with two throughgoing rings of the Procellarum basin (pl. 3; fig. 11.1). The apparent double-basin structure of Tranquillitatis (Stuart-Alexander and Howard, 1970) results from impingement of the older and younger rings on the outline of Tranquillitatis.

Mare Tranquillitatis contains northern and southern belts of the intermediate-age group of Upper Imbrian basalt, separated by a belt of the young age group (pl. 9). Most of the central belt and the western parts of all three belts are of a blue spectral type that is more extensive here than in any other mare (pl. 4; table 5.1). The eastern parts of the northern and southern belts, however, are spectrally red. Sinus Amoris (fig. 9.11) contains thin highly cratered material that is bright and spectrally red. The southeast sector of Mare Tranquillitatis contains similar spectrally red or mottled material, whose wavy topography and degraded superposed craters lend a terralike appearance (Carr, 1970; Wilhelms, 1970a; Wilhelms and McCauley, 1971), but which result from a very thin cover of mare basalt on elevated basin structure (Wilhelms, 1972a). Depths of buried craters also indicate that the eastern Tranquillitatis basalt section is thinner than the western (fig. 5.21*B;* De Hon and Waskom, 1976). These differences correlate with a position in the Procellarum basin: thick and blue closest to the center, thin and red nearer the edge (pl. 4). Units of both age groups, as well as the west basin margin, are cut by arcuate rilles (figs. 6.11, 11.1).

The unique mare-ridge feature Lamont (fig. 11.1) has elicited considerable comment and has been diversely interpreted. It consists of both concentric and radial ridges (Morris and Wilhelms, 1967), is very conspicuous at low Sun elevations, has a small mascon (Scott, 1974; Dvorak and Phillips, 1979), and lies athwart a ring of the Procellarum basin (pl. 4; fig. 11.9; Whitaker, 1981). I suggest that a premare crater perched on this ring created the circular part of the ridge pattern, contains sufficient basalt to appear as a mascon, and remained elevated while subsidence crumpled the surrounding basalt flows into a radial ridge pattern.

Apollo 11 samples

The first rocks returned from the Moon are among the oldest mare-basalt samples. Apollo 11 landed in the southern intermediate-age belt on the oldest of three geologic units mapped near the landing site (figs. 9.8, 11.1, 11.10; Grolier, 1970a, b). Most of the samples obtained presumably came from this unit or from still older buried units. A crater frequency between those for the Fra Mauro Formation and the Apollo 15 mare (table 11.1) and a D_L value of 335 ± 55 m (Boyce, 1976) place the surface unit in the intermediate-age group mapped here (pl. 9). A nearby, older unit that was also dated by crater frequencies (table 11.1) has not been definitely correlated with any samples.

The landing point of the Lunar Module *Eagle* was about 400 m west of the 180-m-wide, 30-m-deep crater "West" between blocky rays of that Copernican crater (figs. 11.10*B*, 11.11; Shoemaker and others, 1969a; Schmitt and others, 1970). Thickness of the regolith is estimated at 3 to 6 m (fig. 11.12; Shoemaker and others, 1970). Beaty and Albee (1978, p. 431–432; 1980) suggested that almost all the samples were derived from the ejecta of West crater and thus came from no more than 30 m deep (fig. 11.12). Because most of the samples were exposed to the space environment for about 0.1 aeon (Eberhardt and others, 1970; Guggisberg and others, 1979), West is probably about 0.1 aeon old. At least one sample (10050) has an exposure age of about 0.5 aeon and thus was probably excavated by a crater older than West, possibly from a basalt unit distant from the landing site (Beaty and Albee, 1978, p. 431–432; 1980).

The returned basalt is characterized by its high Ti content. This property calibrated the telescopic spectral data (McCord, 1969) and showed that blue spectra indicate abundant Ti (Adams and McCord, 1970; McCord and Johnson, 1970). This Ti is contained in several modal minerals, mostly ilmenite (10–17 volume percent; James and Jackson, 1970).

Two types of basalt were recognized by megascopic differences during the first examination of the rock-size samples (larger than 1 cm) and were referred to as types A and B (U.S. National Aeronautics and Space Administration, 1969, p. 123–126; Schmitt and others, 1970). These two basalt types have proved to be distinct in composition, microscopic texture, and initial Sr-isotopic ratios as well. They also differ in crystallization age and display the largest spread in ages from any mare-sampling site.

Low-K, high-Ti.—Most basalt that was called type B in the original classification appears medium-grained and vuggy in hand specimen and ophitic or subophitic in thin section (compare fig. 2.6*A*). It is commonly referred to as Apollo 11 ophitic ilmenite basalt (James and Jackson, 1970) or Apollo 11 low-K basalt. Of the 10 rock samples of this compositional group, 7 have been well dated at from 3.66 to 3.85 aeons by the Ar-Ar method (table 11.3; Guggisberg and others, 1979). Although the Rb-Sr method is less reliable for low-K rocks, the ages

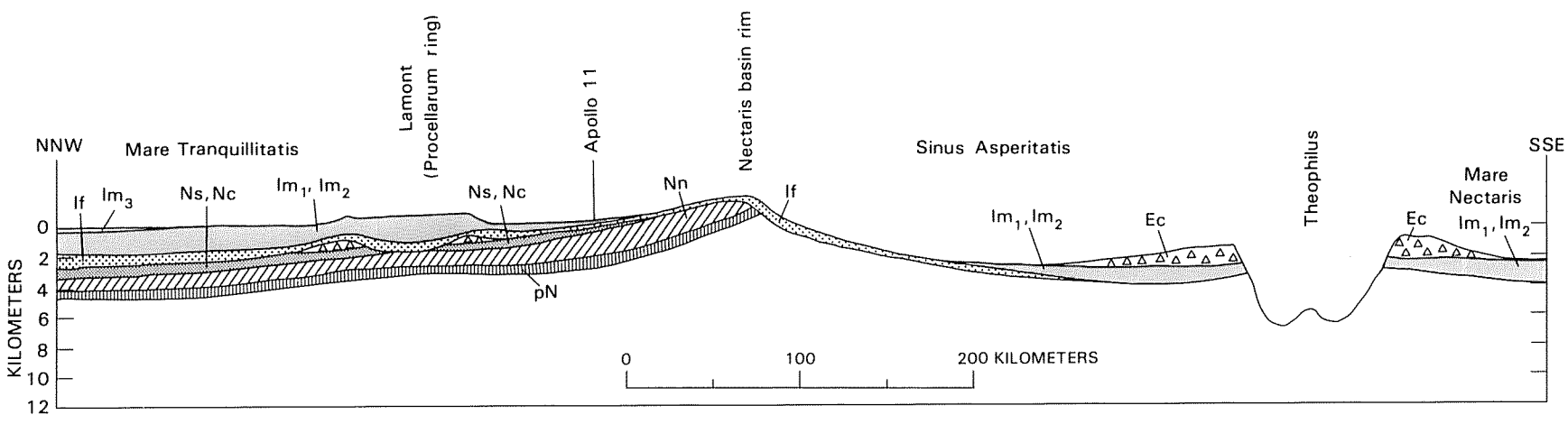

FIGURE 11.9.—Inferred geologic cross section in southern Tranquillitatis basin, Sinus Asperitatis, and Nectaris basin, drawn approximately from top to bottom of figure 11.1, with a southward extension. Units, from oldest to youngest: pN, pre-Nectarian basin, crater, and volcanic deposits, undivided; Nn, Nectaris-basin primary ejecta; Ns and Nc, primary and secondary ejecta of Serenitatis and Crisium basins; If, Fra Mauro Formation (Imbrium-basin ejecta); Im_1, Im_2, and Im_3, Upper Imbrian mare basalt; Ec, Theophilus ejecta. Lamont is drawn as a buried Nectarian crater superposed on a ring of Procellarum basin. An inner ring of Nectaris basin passes under Theophilus, thinning the basalt units. Vertical scale approximate; Theophilus measurements from Pike (1980b).

obtained by the Lunatic Asylum of the California Institute of Technology agree approximately with the Ar-Ar ages, as does one Sm-Nd age (table 11.3; Papanastassiou and others, 1977). Textures, modal mineralogy, and compositions differ sufficiently within the sample group to indicate at least three separate flows (fig. 11.12; Beaty and Albee, 1978). Ar-Ar ages suggest at least four flows (table 11.3; Geiss and others, 1977; Guggisberg and others, 1979), or three flows and an ejecta blanket containing sample 10050 (Beaty and Albee, 1980). Averages of the best Ar-Ar age determinations for each of these four units, performed on plagioclase separates where available, are 3.84, 3.79, 3.70, and 3.67 aeons.

An early conclusion that sample 10003 is older than the average for the compositional group (Turner, 1970) has been confirmed and extended to samples 10029 and 10062 (table 11.3). The 3.84 ± 0.03-aeon average Ar-Ar age obtained for plagioclase separates from samples 10003 and 10029 is close to the 3.85 ± 0.03-aeon age of the Imbrium basin, and the Rb-Sr and Sm-Nd ages of 10062 are older than 3.85 aeons. A pre-Imbrian age is unlikely, however, because Imbrium ejecta is evidently thicker on the adjacent terra than the total 30-m-thick basalt section from which the samples are believed to have been derived (Beaty and Albee, 1980). Also, the error ranges for all age determinations on the older basalt samples and the Imbrium

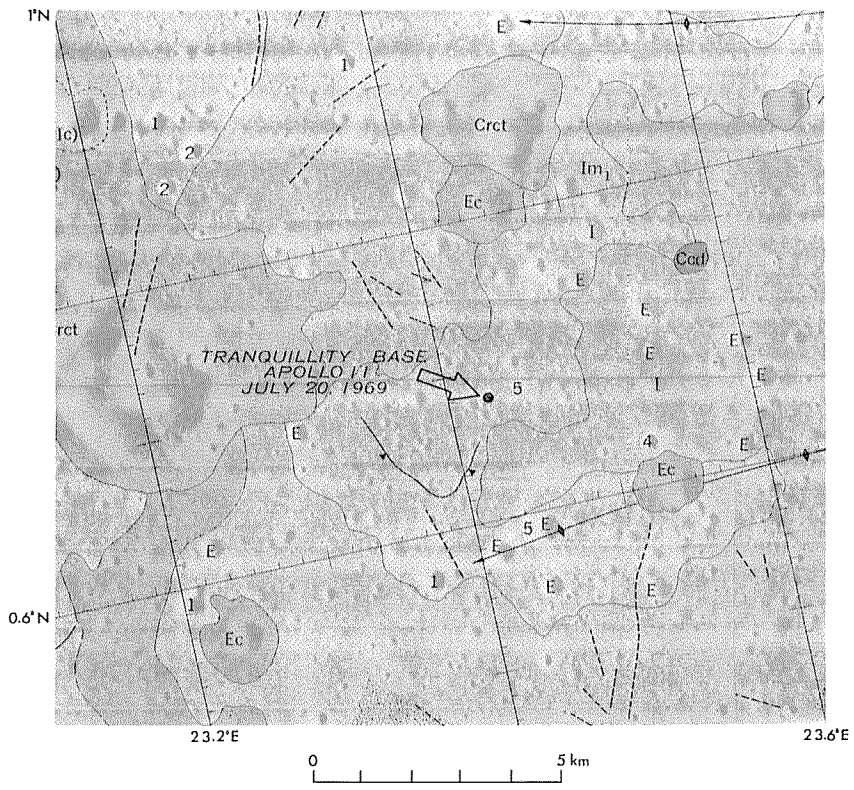

FIGURE 11.10.—Geologic maps of region of Apollo 11 landing site.

A. General region (Grolier, 1970b). Units, from oldest to youngest: Im_1, older Imbrian mare material, surrounded by younger mare unit (unsymbolized here); both units are parts of intermediate-age Upper Imbrian unit as defined in this chapter; Ec, Eratosthenian crater material; Ccd, Copernican "dimple crater" material; Crct, ray-cluster (secondary) craters of Theophilus. Small craters not separately mapped are indicated by letters (E) and numbers (1, 2, 5) corresponding to scheme of N.J. Trask (see chap. 7; figs. 7.12–7.14). Barbed arrows and dashed lines indicate minor mare topography.

B. Detailed map (Grolier, 1970a). Cc_5, young Copernican crater "West" (5 in *A*); heavy dashed line delimits greatest concentration of ejected blocks. Ec and low-numbered Cc, older craters; Cch, material of irregular crater chain (probably secondary); Im, same as in *A*.

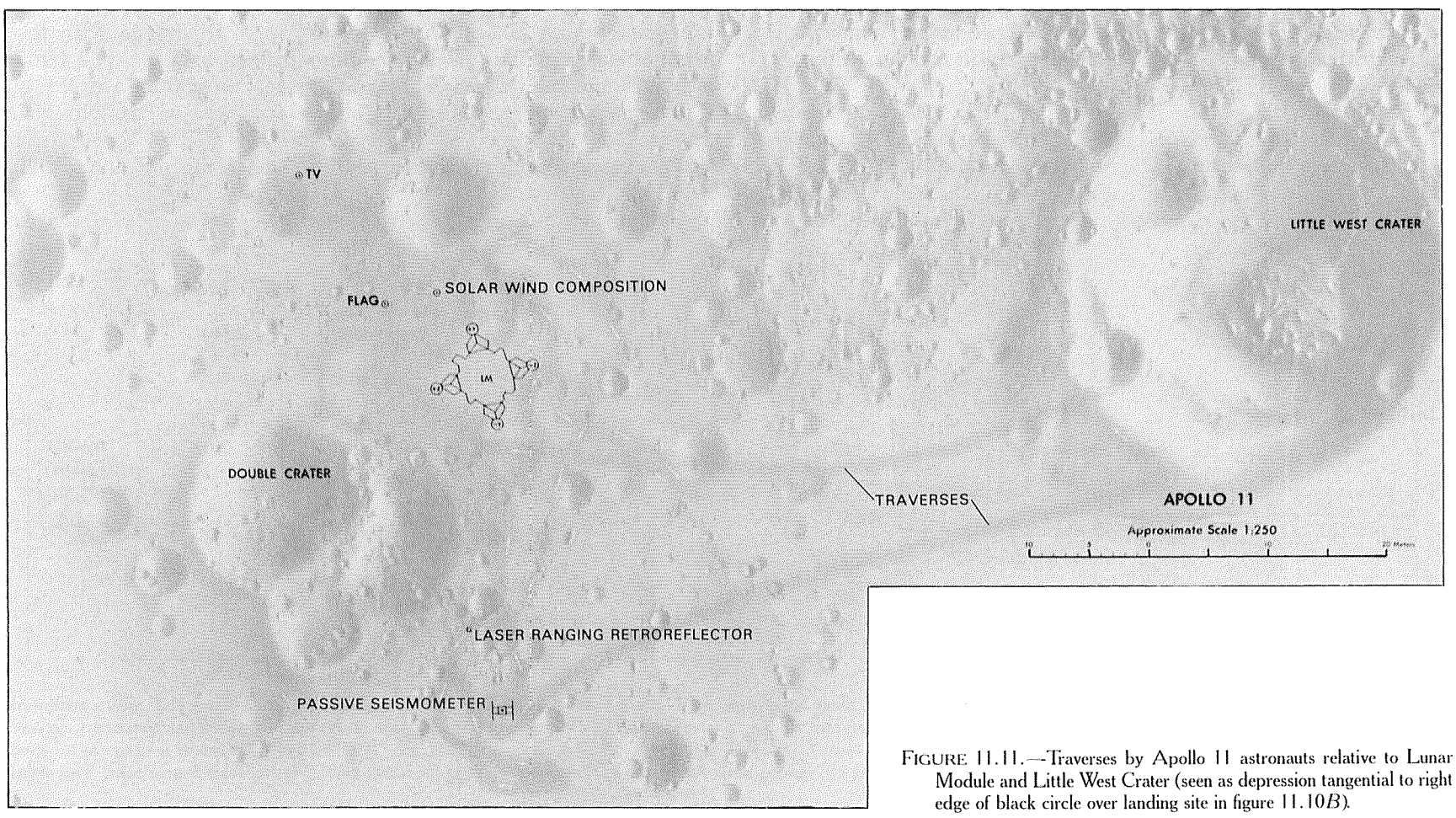

FIGURE 11.11.—Traverses by Apollo 11 astronauts relative to Lunar Module and Little West Crater (seen as depression tangential to right edge of black circle over landing site in figure 11.10*B*).

TABLE 11.3.—*Radiometric ages of large Upper Imbrian basalt samples and pyroclastic glasses*

[Types of samples: (r), small sample collected by rake. Apollo 11 stratigraphic classification after Beaty and Albee (1978, 1980; see fig. 11.12). Apollo 17 chemical classification after Rhodes and others (1977). Stations: LM, vicinity of landed Lunar Module. Apollo 15 stations (fig. 10.9): 1, Elbow Crater; 2 and 7, Apennine front; 3 and 8, on mare; 4, Dune Crater; 9A, rim of Rima Hadley. Apollo 16 station 6, base of Stone Mountain (fig. 9.9; Ulrich and others, 1981). Apollo 17 stations (fig. 9.17; Wolfe and others, 1981): 1, 1 km south of LM; 4, rim of Shorty Crater, 4.3 km west of LM; 5, 1.3 km west of LM; 9, 2 km northeast of LM. All Luna 16 and 24 samples were collected as regolith particles in a single core tube.
References: A80, Alexander and others (1980); AD74, Alexander and Davis (1974; incorporates revisions of earlier determinations by the same laboratory [University of California, Berkeley], which are not given here); B81, Basaltic Volcanism Study Project (1981, p. 950-952, table 7.3.1); BA73, Birck and Allegre (1973); D73, de Laeter and others (1973; reports revisions of earlier determinations by the same laboratory [Australian National University], which are not given here); D78, DePaolo and others (1978); E73, Evensen and others (1973); E73a, Eberhardt and others (1973a); G79, Guggisberg and others (1979); H72, Huneke and others (1972); H73, Huneke and others (1973); H74, Huneke and others (1974); H75, Horn and others (1975); H78, Huneke (1978); HS73, Husain and Schaeffer (1973); Hs74, Husain (1974); J75, Jessberger and others (1975); K73a, Kirsten and others (1973a); KH74, Kirsten and Horn (1974); L75, Lugmair and others (1975); L78, Lunatic Asylum (1978); M71, Murthy and others (1971); M72, Murthy and others (1972); MC76, Murthy and Coscio (1976); N74, Nyquist and others (1974); N75, Nyquist and others (1975); N76, Nyquist and others (1976; see also Nyquist, 1977); N79a, Nyquist and others (1979a); P70, Papanastassiou and others (1970); P72, Podosek and others (1972); P77, Papanastassiou and others (1977); PH73, Podosek and Huneke (1973); PW71a, Papanastassiou and Wasserburg (1971a); PW72a, Papanastassiou and Wasserburg (1972a); PW73, Papanastassiou and Wasserburg (1973); PW75, Papanastassiou and Wasserburg (1975); S73, Stettler and others (1973); S74, Stettler and others (1974); S78, Schaeffer and others (1978); SA78, Stettler and Albarede (1978); SA79, Saito and Alexander (1979); SH73, Schaeffer and Husain (1973); SS77, Schaeffer and Schaeffer (1977); T73, Tatsumoto and others (1973); T74, Tera and others (1974); Tu70, Turner (1970); Tu71, Turner (1971); Tu73, Turner and others (1973); TC74, Turner and Cadogan (1974); TC75, Turner and Cadogan (1975; see also Turner, 1977); TW75, Tera and Wasserburg (1975); TW76, Tera and Wasserburg (1976); Y72, York and others (1972). There is some question whether the values obtained by HS73, Hs74, S78, SH73, and SS77 should be altered in accord with the decay constants recommended by the International Union of Geological Sciences [IUGS] (Steiger and Jäger, 1977; see table 9.1, headnote); the recalculated values are listed here and in B81 for these and all other samples. p, analysis performed on plagioclase mineral separates and considered to be superior.
Other methods: Sm, Sm-Nd; U, U-Pb-Th]

Group	Sample	Type	Station	Rb-Sr age (aeons)	Reference	Ar-Ar age (aeons)	Reference	Other age (aeons)	Method	Reference
Apollo 15 green glass.	15086	---	1	----------		3.25±0.06	H74	----------		
	15426	---	7	----------		3.34±0.06	PH73	----------		
Apollo 15 olivine basalt.	15016	---	3	3.22±0.05	E73	3.34±0.08	B81	----------		
	15385	(r)	7	----------		3.35±0.05	Hs74	----------		
	15555	---	9A	3.23±0.08	M72	3.22±0.03	AD74	3.3	U	TW75
		---	---	3.25±0.04	PW73	3.24±0.06	Hs74	----------		
		----------				3.27±0.03	P72 (p)	----------		
		----------				3.27±0.06	Y72	----------		
		----------				3.29±0.04	Hs74	----------		
	15607	(r)	9A	----------		3.23±0.12	Hs74	----------		
	15633	(r)	9A	----------		3.22±0.05	Hs74	----------		
	15659	(r)	9A	----------		3.30±0.04	Hs74	----------		
	15668	(r)	9A	----------		3.10±0.05	Hs74	----------		
	15678	(r)	9A	----------		3.34±0.05	Hs74	----------		
	15683	(r)	9A	----------		3.32±0.03	Hs74	----------		
Apollo 15 pigeonite basalt.	15058	---	8	----------		3.32±0.03	Hs74	----------		
	15065	---	1	3.21±0.04	PW73	----------		----------		
	15075	---	1	----------		3.41±0.20	SS77	----------		
	15076	---	1	3.26±0.08	PW73	3.31±0.04	S73	----------		
	15085	---	1	3.33±0.04	PW73	----------		----------		
	15117	(r)	2	3.28±0.04	PW73	----------		----------		
	15499	---	4	----------		3.30±0.08	Hs74	----------		
	15682	(r)	9A	3.37±0.07	PW73	----------		----------		
Luna 24 VLT basalt.	24077,13	----------				3.33±0.21	S78	----------		
	24077,63	----------				3.26±0.06	S78	----------		
	24170	----------				3.30±0.04	L78	3.30±0.05	Sm	D78
		----------				3.33±0.20	B81	----------		
	L24A	----------				3.61±0.12	SA78	----------		
Luna 16 feldspathic basalt.	L16-B1	---	---	3.35±0.18	PW72a	3.41±0.04	H72	----------		
		---	---	3.4±0.2	BA73	----------		----------		
Apollo 17 orange-and-black glass.	74001	OB	4	----------		3.65±0.02	SA79	----------		
	74220	OB	4	----------		3.50±0.05	H73	3.48±0.03	U	TW76
		----------				3.60±0.04	H78	3.63	U	T73
		----------				3.66±0.03	A80	----------		
		----------				3.66±0.06	HS73	----------		
		----------				3.55-3.66	E73a	----------		
Apollo 17 low-K, high-Ti basalt.	70017	U	LM	3.60±0.18	N75	----------		----------		
	70035	U	LM	3.65±0.11	N74	3.69±0.07	S73	----------		
		---	---	3.74±0.06	E73	----------		----------		
	70135	U	LM	3.67±0.09	N75	----------		3.76±0.06	Sm	N79a
	70215	B	LM	----------		3.79±0.04	KH74	----------		
	70255	A	LM	----------		3.79±0.02	SS77	----------		
	71055	U	1	3.56±0.09	T74	----------		----------		
	74255	C	4	3.62±0.12	MC76	----------		----------		
		---	---	3.75±0.06	N76	----------		----------		
	75035	A	5	3.73±0.14	MC76	3.71±0.05	TC75	----------		
	75055	A	5	3.69±0.06	T74	3.71±0.05	Tu73	----------		
		----------				3.73±0.04	H73	----------		
		----------				3.77±0.05	K73a	----------		
	75075	U	5	3.74±0.06	MC76	3.67±0.06	J75	3.70±0.07	Sm	L75
		---	---	3.75±0.10	T73	3.69±0.02	H75	----------		
		---	---	3.76±0.12	N75	----------		----------		
	79155	U	9	----------		3.75±0.04	KH74	----------		
Apollo 16 feldspathic basalt.	66043,2, 17	---	6	----------		3.74±0.05	SH73	----------		
Apollo 11 high-K, high-Ti basalt.	10017	A	LM	3.51±0.05	P70	----------		----------		
	10022	A	LM	----------		3.54±0.06	G79	----------		
		----------				3.54±0.09	Tu70	----------		
	10024	A	LM	3.53±0.07	PW71a	----------		----------		
	10031	A	LM	----------		3.55±0.08	G79	----------		
	10032	A	LM	----------		3.53±0.06	G79	----------		
	10057	A	LM	3.55±0.04	P70	----------		----------		
	10069	A	LM	3.60±0.06	P70	----------		----------		
	10071	A	LM	3.60±0.02	P70	3.47±0.06	S73 (p)	----------		
	10072	A	LM	3.56±0.05	P77	3.48±0.05	Tu70	3.57±0.03	Sm	P77
		---	---	3.63±0.11	D73	3.57±0.05	G79 (p)	----------		
Apollo 11 low-K, low-Ti basalt.	10044	B1	LM	3.63±0.11	P70	3.66±0.04	G79	----------		
		----------				3.68±0.05	Tu70	----------		
	10047	B1	LM	----------		3.69±0.03	S74, G79	----------		
	10058	B1	LM	3.55±0.11	M71	3.66±0.04	G79	----------		
		---	---	3.55±0.22	P70	----------		----------		
	10020	?	LM	----------		3.72±0.04	G79	----------		
	10050	?	LM	----------		3.70±0.03	G79 (p)	----------		
	10062	B2?	LM	3.92±0.11	P77	3.77±0.06	Tu70	3.88±0.06	Sm	P77
		----------				3.79±0.04	G79 (p)	----------		
	10003	B2	LM	3.76±0.08	PW75	3.85±0.03	S74 (p)	----------		
		----------				3.86±0.07	Tu70	----------		
	10029	B2	LM	----------		3.83±0.03	G79 (p)	----------		

basin overlap and are large for the Rb-Sr and Sm-Nd ages. The 3.84 ± 0.03-aeon average Ar-Ar age of the plagioclase separates is probably close to the actual age of the flow (barring systematic errors in all Ar-Ar ages). Extrusion of the low-K, high-Ti basalt probably began soon after the Imbrium impact (fig. 11.9). A pre-Orientale (Early Imbrian) age is possible because Orientale ejecta may well be absent or very thin here.

High-K, high-Ti.—The other type of basalt (originally, type A) is richer in K_2O, as well as in TiO_2, Na_2O, CaO, and Al_2O_3, than the low-K group (Papike and others, 1976). Grain sizes are finer than those of the low-K group, and textures are commonly intersertal (unoriented crystal grains separated by small amounts of glass or crystallized glass); accordingly, the group is also called Apollo 11 intersertal ilmenite basalt (James and Jackson, 1970). For this sample group, Rb-Sr ages are more reliable than Ar-Ar ages (Stettler and others, 1974; Papanastassiou and others, 1977). Six rocks have been dated by this method (table 11.3). Rb-Sr ages from any single laboratory cluster tightly (for example, Papanastassiou and others, 1970, 1977). This consistency and the data on textures and bulk compositions are consistent with derivation of all the rocks of this type from a single flow (Papike and others, 1976; Beaty and Albee, 1978, 1980); only minor fractionation near the surface (Papike and others, 1976) or in shallow magma chambers (Beaty and Albee, 1978) is indicated. Most Ar-Ar ages are younger than the Rb-Sr ages, probably because argon was lost after crystallization (Turner, 1977). The average of the best Rb-Sr ages and the Sm-Nd age is 3.57 aeons.

Exposure ages (duration of exposure to cosmic rays) of the two compositional groups differ and have been interpreted as indicating that the high-K flow is the uppermost sampled flow and overlies the low-K flows (Eberhardt and others, 1970; Beaty and Albee, 1980), in accord with the absolute ages (fig. 11.12). Origin of the two basalt types from different magma reservoirs is indicated by the different initial Sr-isotopic ratios (Papanastassiou and others, 1977). I tentatively correlate the frequency of 3.4×10^{-3} craters at least 1 km in diameter per square kilometer and the D_L value of 335 m listed in table 11.1 (both with large error bars) with the high-K flow.

Summary and interpretation

If the source section of all the samples is, indeed, only 30 m thick, an incredibly low extrusion rate of one flow averaging 6 m in thickness every 54 million years is indicated. Other deposits presumably underlie the sampled flows because the mare surface here is relatively unbroken by islands belonging to buried craters or other terra (fig. 11.1). Nonetheless, a thick section of Upper Imbrian flows is unlikely, considering the very old age, within the Imbrian System, of some of the lavas that were sampled. Therefore, Lower Imbrian, Nectarian, and pre-Nectarian deposits must be present in the subsurface (fig. 11.9). These deposits include thick ejecta of the nearby Nectaris basin, thinner deposits from the Serenitatis and Imbrium basins, and possible deposits of the Crisium and Orientale basins. Pre-Nectarian, Nectarian, and Lower Imbrian basalt flows may be interbedded with this ejecta sequence. Regoliths formed by smaller craters (not shown in fig. 11.9) separate all the deposits in proportion to the timespan each was exposed to the surface.

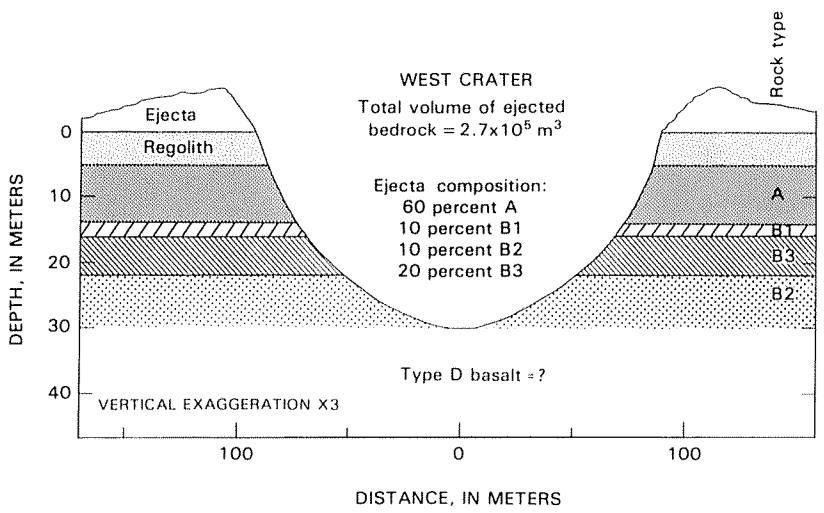

FIGURE 11.12.—Inferred basalt stratification penetrated by West Crater and yielding the Apollo 11 samples (after Beaty and Albee, 1980). A, high-K, high-Ti basalt; B1, B3, and B2, flows of low-K, high-Ti basalt (Beaty and Albee, 1978). B1 may be ejecta blanket. No definite B3 basalt is listed in table 11.3; samples 10050 and 10062 may be part of that flow (Beaty and Albee, 1978). Type D, possible additional basalt type not dated or discussed here.

Basalt extrusion was also relatively sluggish in the rest of Mare Tranquillitatis during the Late Imbrian Epoch. Although interbedded basalt flows and ejecta may reach a thickness of 1.25 km in one spot, most of the total section is thin (fig. 5.21*B*; De Hon and Waskom, 1976). Two somewhat indistinct color and age units are present.

In summary, the most recent history of Mare Tranquillitatis is characterized by thin and slowly extruded, yet areally extensive, lavas of intermediate and late Late Imbrian age. The western flows are thicker and richer in Ti than the eastern, except that some eastern flows of the young Late Imbrian group are also Ti-rich.

MARE NECTARIS

General stratigraphy

Mare Nectaris differs markedly from Mare Tranquillitatis. Although the Nectaris basin is much younger and slightly larger than the Tranquillitatis basin (860 versus 800 km diam), mare volcanism was even more sluggish. Nectaris is much the smaller mare (table 6.1). Little or no basalt of the young Late Imbrian group is present (pl. 9; fig. 11.9; Boyce, 1976; Whitford-Stark, 1981). The Nectaris basalt has subsided enough to open only a few arcuate grabens on the west margin of the mare (pl. 5). The spectral class (mBG-, table 5.1) indicates intermediate values of the spectrally measured properties. Orbital geochemical data are not available except in the narrow neck, Sinus Asperitatis, that connects Nectaris with Tranquillitatis (figs. 11.1, 11.9), and there the surface is contaminated by Theophilus ejecta. The Asperitatis basalt section is as thick as or thicker—possibly 1.5 km—than those in central Nectaris and Tranquillitatis (fig. 5.21*B*; De Hon and Waskom, 1976). It even coincides with a small mascon (Scott, 1974).

Apollo 16 samples

Although it did not land near a mare and was not designed to sample mare materials, Apollo 16 returned a few fragments of mare basalt. They were presumably thrown to the sampling site in the ejecta of an impact crater, probably Theophilus, in which case their source is Mare Nectaris (fig. 11.1; Delano, 1975). The fragments include both Ti- and Al-rich types. Ar-Ar analysis of one Ti-rich sample yielded an age of 3.74 aeons, consistent with the photogeologically old age of most of Mare Nectaris (table 11.3; Schaefer and Husain, 1973).

Summary and interpretation

The differences in age and position relative to the Procellarum basin between the Nectaris and Tranquillitatis basins may account for the differences between Maria Nectaris and Tranquillitatis. First, the fact that Mare Tranquillitatis is extensive, yet relatively thin (table 6.1; fig. 5.21*B*; De Hon and Waskom, 1976), probably results from premare leveling of the basin floor by thick Nectaris-basin and other ejecta deposits and, possibly, by pre-Imbrian basalt (fig. 11.9). Second, the thick lithosphere outside Procellarum may have prevented sufficient subsidence to erase the Nectaris mascon, to open large grabens, or to provide much space for basalt extrusion. Each condition was opposite in Tranquillitatis, where the weak lithosphere allowed extensive basalt extrusion and subsidence. This hypothetical significance of lithospheric differences is supported by the relatively extensive mare development in Sinus Asperitatis, which is outside the centers of Nectaris and Tranquillitatis but inside the rim of the Procellarum basin (pl. 4).

MARE SERENITATIS

General stratigraphy

Whereas Serenitatis is among the Moon's least well understood basins (see chap. 9), Mare Serenitatis displays clear stratigraphic and structural relations that have made it a model for other maria (Carr,

FIGURE 11.13.—Southeast border of Mare Serenitatis. Young light-colored basalt of mare center sharply abuts older dark mare and dark-mantling materials (white arrows). Older units are faulted (compare fig. 6.2). Black arrow, rilles and endogenic craters shown in figure 5.10A. Rayed Copernican crater below black arrow is Dawes (18 km, 17° N., 26° E.). Apollo 17 landing site is visible in right-hand frame (black-and-white arrow; compare fig. 9.13). Stereoscopic pairs of Apollo 17 frames M–5000, M–5002, and M–5004 (from right to left).

1966a; Howard and others, 1973; Thompson and others, 1973; Muehlberger, 1974; Head, 1979c; Solomon and Head, 1979). The southeast margin contains a continuation of the intermediate-age, dark, spectrally blue unit that characterizes northwestern Mare Tranquillitatis. This border zone is faulted by conspicuous arcuate grabens (pls. 4, 5, 9; figs. 5.17, 6.2, 11.13). The southwest-marginal unit is younger (pl. 9; Howard and others, 1973), of a similar but less blue spectral class (hDWA, pl. 4), and unfaulted. The division between the two units falls along the middle ring of the Procellarum basin (pl. 4). The center of Mare Serenitatis is occupied by younger, relatively bright material of spectral class mISP (table 5.1), which, under the designation "MS–2," is the standard for normalizing color spectra (fig. 5.19). This red or "orange" material appears to be spectrally uniform even though it consists of numerous small flows (not mapped here). The central units are not cut by grabens but contain large mare ridges (see chap. 6; Muehlberger, 1974; Maxwell and others, 1975; Solomon and Head, 1979).

In early work, the dark units were thought to be the younger (Carr, 1966a, b), partly because the central mare seemed in telescopic photographs to have more craters than the border mare. Along the east and west margins, this relation has been confirmed; the dark border units there (spectral class hDWA, pl. 4) are younger than the light (pl. 10). Stereoscopic spacecraft photographs have shown, however, that the central mare is younger than the southeast- and southwest-border units; it sharply abuts most of the raised border zone and transects the rilles (figs. 5.16, 6.2, 11.13; Howard and others, 1973). The apparent abundance of craters in the central mare results from their greater brightness and sharpness, which properties are caused by excavation of fresh rock through the thinner regoliths on the younger lavas (Young, 1975); the older border mare has more large, subdued craters.

Serenitatis is a massive mare. The 1-km isopach encloses a large part of the mare (fig. 5.21*B*; table 6.1), and the radar-sounder and mascon data suggest depths of more than 2 km (see chap. 5). The large massive load of basalt depressed the basin and the earlier Ti-rich basalt and opened the many arcuate grabens (chap. 6; fig. 6.2; Muehlberger, 1974; Solomon and Head, 1979, 1980). Serenitatis, therefore, differs considerably from the maria already described. Its basalt units are strongly deformed, spectrally distinct, sharply divergent in age, thick, and extensive relative to basin size (figs. 11.13, 11.14).

Apollo 17 samples

The largest suite of lunar mare basalt was returned by Apollo 17, despite the emphasis of this last Apollo mission on the Serenitatis-basin massifs (see chap. 9). The landing site was on the dark floor of a marginal embayment of Mare Serenitatis called the Taurus-Littrow Valley (figs. 9.13, 11.13, 11.15; Wolfe and others, 1981). The "subfloor basalt" may be as thick as 1.4 km (Cooper and others, 1974); the returned samples were excavated by craters from as much as 100 m below the surface (fig. 11.15; Wolfe and others, 1981). They are as rich as or richer in TiO_2 than the Apollo 11 basalt samples and are generally similar petrologically. Two main types were at first recognized on the basis of major-element composition (Papike and others, 1976): (1) a dominant mafic Mg-rich olivine basalt especially rich in Ti (max 14 weight percent TiO_2), and (2) a less abundant, coarse-grained basalt very similar to the Apollo 11 low-K, high-Ti variety. The second type was obtained from the rim of the largest sampled crater, Camelot, 650 m in diameter (sta. 5), and thus may have lain at the greatest depth of all the sampled basalt—possibly deeper than 100 m (Wolfe and others, 1981, p. 109–114, 204–205).

Subsequent examination of a larger sample suite by Rhodes and others (1976) and Warner and others (1979) disclosed that the gaps in major-element composition are occupied and led to a fourfold classification into types A, B, C, and an unclassified type U that is based more on trace elements. These authors suggested that the coarse-grained, low-K, relatively low-Ti basalt from the Camelot rim was not derived from a separate magma but is a highly fractionated form of the type A basalt. Other type A materials are scattered over the collection area. Type B basalt was collected mostly in the east half of the collection area, especially in ejecta of the 600-m-diameter crater Steno (sta. 1). These rocks may have lain somewhat above the source of the Camelot samples (Wolfe and others, 1981, p. 35, 205). Type C basalt, the rarest and most distinctive, was collected only from the rim of the 110-m-diameter crater Shorty (sta. 4) and thus probably

was derived from the shallowest depths (fig. 11.15). The mostly coarse-grained type U rocks came from all parts of the collection area and are the most numerous of the rock-size samples that were dated (table 11.3).

Rhodes and others (1976) suggested that each of the three basalt types A, B, and C differs sufficiently from the others to indicate extrusion as a separate lava flow. Variation within each type and, probably, among some or all of the type U rocks arose by fractional crystallization of one of the magmas on or near the surface.

The scatter in the absolute ages is so great (table 11.3) that no firm correlations with the A-B-C stratigraphic sequence or composition have been proposed. The Ar-Ar ages range from 3.67 to 3.79 aeons, and the Rb-Sr ages from 3.56 to 3.76 aeons; two Sm-Nd ages are 3.70 and 3.76 aeons (table 11.3). The average of the ages obtained by all methods having stated error ranges less than 0.1 aeon is 3.72 aeons. The absence of obvious correlations among age, composition, and sampling locality suggests that all the Apollo 17 basalt was extruded within a short time. The age of 3.72 aeons is, therefore, tentatively accepted here as the emplacement age of the entire sequence, more than 100 m thick. Partial melting of a heterogeneous source in a small zone of the mantle is indicated by the small ranges in age and composition (Rhodes and others, 1976).

A major Apollo 17 mission objective was to sample the dark-mantling materials, which were believed to be young (Scott and others, 1972; Hinners, 1973). They were recovered in the form of orange and black glass droplets ("beads") with a mean diameter of 0.04 mm. This material, which composes from a few percent to 20 percent of the regolith, was recovered in greater concentrations from the rim of the 19-million-year-old (Eugster and others, 1977) crater Shorty (Muehlberger and others, 1973; Heiken and others, 1974; Wolfe and others, 1975, 1981). Shorty's ejecta appears dark from orbit and black and orange on the surface. Orange droplets compose a bed, about 25 cm thick, overlying a bed of black droplets. The color difference of these droplets, whose compositions are the same, is due to more nearly complete crystallization of the black (Haggerty, 1974; Heiken and others, 1974). The devitrified black beads have a blue spectrum, and the glassy orange beads a red spectrum (Adams and others, 1974; Pieters and others, 1974). Presumably, the degree of devitrification accounts for similar spectra elsewhere, such as the red spectra (and orange-brown visual appearance) of the dark-mantling materials on the Aristachus Plateau (Zisk and others, 1977).

The telescopic spectrum of "pure" dark-mantling materials north of the Apollo 17 landing site is similar to the laboratory spectrum of the droplets from Shorty but is only partly like that of droplets from the regolith around the landing site (Adams and others, 1974). The regolith there probably contains a mixture of true dark-mantling materials, consisting of orange and black glass derived from a sheet originally at least 1.5 m thick, and of Ti-rich fragments derived from the subfloor basalt. The total thickness of the weakly bonded glass-bead deposit plus the regolith is 5 to 28 m, and the mean thickness 14 m (fig. 11.15; Wolfe and others, 1975, 1981).

A pyroclastic rather than an impact origin is indicated by the chemistry and absence of fragments in the glasses and by the distribution of dark-mantling deposits at the margins of several addi-

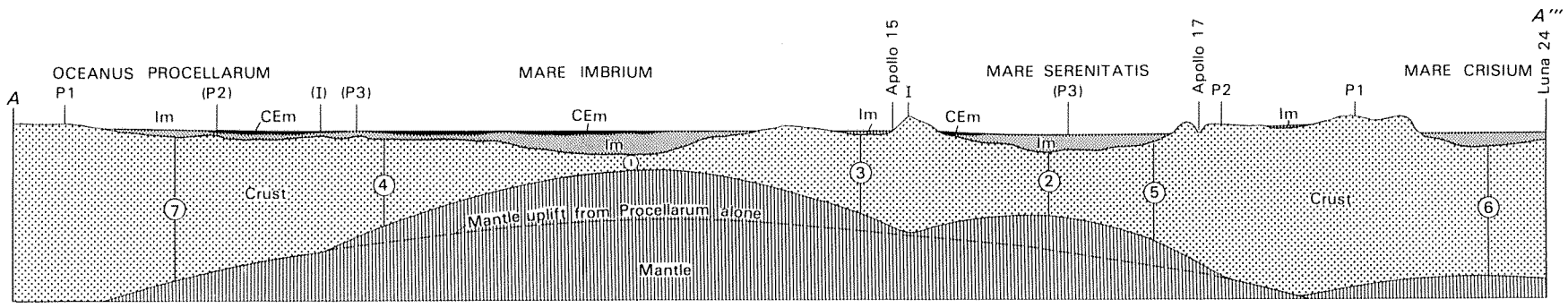

FIGURE 11.14.—Geologic cross section, drawn along line A–A''' in figure 8.4, showing relative depths of mare basalt and inferred shape of crust-mantle boundary; vertical scale arbitrary. P1, P2, and P3, rings of Procellarum basin (pl. 3); I, rim of Imbrium basin; symbols in parentheses, buried rings; Im, Imbrian mare basalt; CEm, Copernican and Eratosthenian mare basalt (pls. 10, 11). Superposed mantle uplifts resulting from superposed basin impacts are indicated diagrammatically; total uplift is thought to depend on crustal thickness remaining after formation of Procellarum basin and on size of superposed basins. Numbers 1 through 7 indicate pathways from mantle source of mare materials to surface at time of eruptions, from shortest to longest.

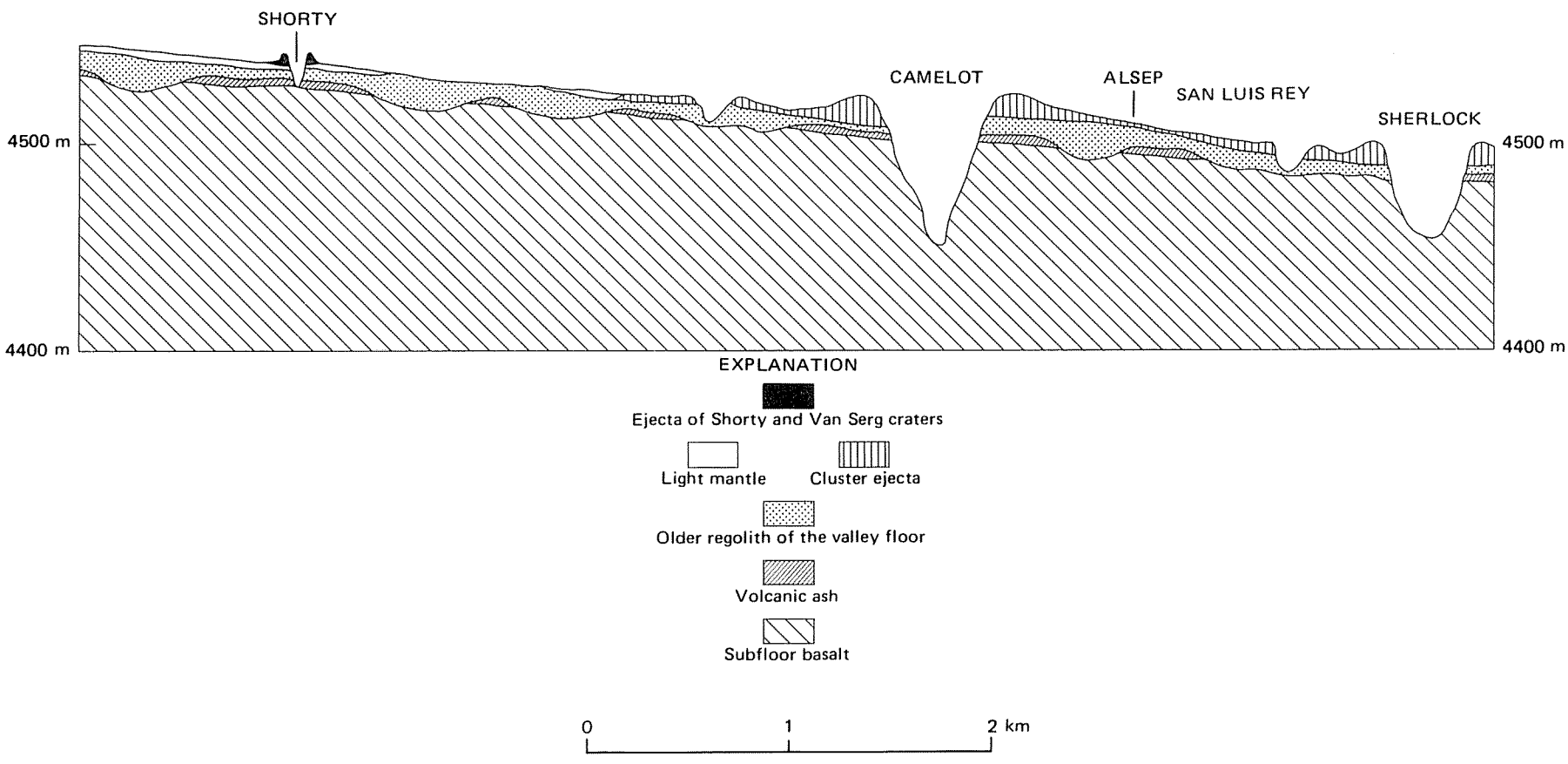

FIGURE 11.15.—Geologic cross section, drawn approximately east-west in area of figure 9.17, showing regolith, mare, and glass-droplet ("volcanic ash") deposits in Taurus-Littrow Valley. Light mantle, landslide from South Massif; cluster ejecta, ejecta of "Central Cluster" craters believed to be secondary to Tycho; ALSEP, Apollo Lunar Surface Experiments Package (mostly geophysical instruments). Vertical elevations above arbitrary datum. From Wolfe and others (1981, fig. 248).

tional maria (Heiken and others, 1974). These glasses apparently were formed during an early "lava fountain" or "fire fountain" stage of mare eruption. At Taurus-Littrow, they were deposited on the subfloor basalt before most of the regolith formed (Head, 1974a; Heiken and others, 1974). The pyroclastic material was probably derived from a different magma than was the sampled basalt (Hubbard and Rhodes, 1976).

Although sampling confirmed the pyroclastic origin of the dark-mantling materials, it refuted estimates of a young age. Determinations of absolute age by different laboratories range from 3.50 to 3.66 aeons (table 11.3); the average of the single determination for sample 74001 and the three best determinations for sample 74220 is 3.64 aeons, and this age is adopted here. All these determinations are consistent with superposition of the orange glass deposit on the subfloor basalt. The low crater density that led to estimates of a young age is due to initially subdued shapes and rapid degradation of impact craters in the noncohesive deposits (Lucchitta and Sanchez, 1975).

Summary and interpretation

The extrusional history of the Apollo 17 basalt was very different from that of its compositional relative, the Apollo 11 basalt. In the Taurus-Littrow embayment, a massive flow or related flows, more than 100 m thick, formed in a time so short that age differences are geochronologically unresolvable. Fountains driven by volatile material spewed forth liquid droplets that accumulated as deposits of glass. More than 100 million years before and after the lavas and pyroclastic materials poured out here, a few meters of basalt were being added to the margin of Mare Tranquillitatis. Then, after both margins were covered by the high-Ti basalt flows, the center of Serenitatis was filled by voluminous low-Ti basalt flows that depressed and faulted the older Ti-rich basalt and the basin. The spectral and stratigraphic uniformity of the many small flows of low-Ti basalt suggests high eruption rates.

Although Maria Serenitatis and Tranquillitatis are similar in area, the volume of Serenitatis is by far the greater—second only to that of Mare Imbrium (fig. 5.21; table 6.1). The voluminous volcanism is due to the relatively young age of the Serenitatis basin (see chap. 9), to its premare filling by only one major deposit (Imbrium ejecta), and, probably, to its superposition on a relatively weak part of the lithosphere relatively near the center of the Procellarum basin (figs. 11.9, 11.14).

MARE FECUNDITATIS

General stratigraphy

The poorly photographed Mare Fecunditatis occupies a pre-Nectarian basin, about 990 km in diameter, outside the Procellarum basin. The mare is shallow, spectrally mottled and bland, relatively aluminous in X-ray readings (Adler and others, 1972; Hubbard, 1979), and apparently middle to late Late Imbrian in age (pl. 9). Like Mare Tranquillitatis, Mare Fecunditatis occupies a large fraction of the basin diameter but is relatively thin (table 6.1). Its west edge is faulted by arcuate grabens.

Selenographically, Mare Fecunditatis includes a subcircular southward extension of the main mare. This second mare, about 250 km in diameter, may occupy an (unmapped) large crater or small basin superposed on the 990-km-diameter Fecunditatis basin. Alternatively, the Fecunditatis impact may have been double.

Luna 16 samples

The Luna 16 unmanned sample-return mission (September 1970) yielded 101 g of small regolith fragments from Mare Fecunditatis (lat 0.7° S, long 56.3° E.; fig. 11.16; McCauley and Scott, 1972). The dominant basalt is a feldspathic, high-Al type distinguished by a high FeO/MgO ratio from other mare basalt, KREEP-rich material, and high-Al mare-basalt clasts from the Apollo 14 breccia (Kurat and others, 1976). The Rb-Sr and Ar-Ar ages agree fairly well at an average of 3.38 aeons, but the Ar-Ar age of 3.41 ± 0.02 aeons has much the smaller error range (table 11.3); a weighted average of 3.40 aeons is adopted here. The sampling site is on a dark unit whose spectral class (hDW-) indicates a higher Ti content than most of Mare Fecunditatis (pl. 4). The Al-rich sample composition is consistent with the orbital detection of relatively high Al/Si ratios for the overflown part of the mare (Hubbard, 1979).

Summary and interpretation

The aluminous composition of the basaltic magmas may have favored their hydrostatic ascent and extrusion through the thick crust in the Fecunditatis region, because they probably are the mare-basalt magmas closest in density to the terra crust (2.8–2.9 g/cm^3; Solomon, 1975). Possibly, Al-rich magmas could be extruded where denser magmas would remain beneath the surface.

Of all the maria considered here that lie outside Procellarum, Mare Fecunditatis occupies the largest percentage of its basin's area (table 6.1). A possible explanation is that the younger Nectaris and Crisium basins "assisted" the volcanism. The grabens in western Fecunditatis lie within the rim of the Nectaris basin (pl. 5). Northern Mare Fecunditatis, including the compositionally anomalous (relatively Ti-rich) Luna 16 material, lies within the proposed 1,060-km-diameter rim of the Crisium basin (pl. 9; fig. 11.16). Therefore, the lithospheric thinning required for mare extrusion and structural deformation is achieved here by superposition of basins other than Procellarum.

MARE CRISIUM

General stratigraphy

Mare Crisium occupies an elliptical area, 420 km north-south by 560 km east-west (pl. 4). The average diameter of this mare is less than half that of the containing Crisium basin in my interpretation (1,060 km; see chap. 9; tables 4.1, 6.1). Crisium is probably between the Serenitatis and Nectaris basins in age, closer to Serenitatis (table 9.3). Mare Crisium has properties in common with both Maria Serenitatis and Nectaris. It has a mascon, as do both of these maria. The basalt section is about as thick as that of Serenitatis and thicker than that of Nectaris (fig. 5.21*B*; De Hon and Waskom, 1976). In respect to its areal extent relative to the basin diameter, however, it more closely resembles Nectaris (if the Crisium basin is indeed as large as I suggest). Tectonically, Crisium is more like Nectaris than Serenitatis because no arcuate grabens have opened since the visible mare formed (pl. 5).

Mare Spumans, Mare Undarum, and other "lakes" surround the main Mare Crisium at considerably higher elevation (fig. 4.9). In chapter 4, this relation was interpreted as analogous to the steplike structure of the Orientale basin and its small superposed maria. The "lakes" are as high as or higher than the adjacent Mare Fecunditatis (fig. 6.23).

Investigative groups led by J.M. Boyce (Boyce and Johnson, 1977; Boyce and others, 1977) and J.W. Head (Head and others, 1978a) mapped several age units, but these two groups did not agree on the units' distribution. Photographs suitable for age determinations are available only in the southern part of the mare under the Apollo 17 orbits. To me, Crisium seems to be among the stratigraphically most uniform maria, and I map it here entirely as part of the youngest of the three Late Imbrian age categories (pl. 9). The "lakes" are older.

Head and others (1978a) and Pieters (1978) mapped several color units in Mare Crisium (pl. 4). An Mg-rich unit similar to the Luna 16 basalt is exposed at the southeast margin (hDWA, pl. 4); this may also be the unit exposed in the ejecta of the crater Picard (fig. 5.23; Andre and others, 1978; Head and others, 1978a). The unit sampled by Luna 24 is the type area of spectral unit LISP. Unit hDWA is moderately rich in Ti, but the other spectral units are relatively poor in Ti and rich in Fe (table 5.1). Hubbard (1979) interpreted data obtained by the orbiting X-ray spectrometer to mean that Mare Crisium is more aluminous than the maria farther west, about equal to Mare Fecunditatis, and less aluminous than only Mare Smythii among the major analyzed maria.

Luna 24 samples

The most recently (August 1976) collected lunar sample is a 160-cm-long drill core obtained from the regolith of Mare Crisium by the

unmanned Soviet spacecraft Luna 24 (lat 12.7° N., long 62.2° E.; fig. 9.3; Butler and Morrison, 1977; Florensky and others, 1977). Most of the basalt fragments are very low in Ti (less than 1.5 weight percent TiO_2), a basalt type previously found only in small amounts in the Apollo 17 drill core (Vaniman and Papike, 1977). The Luna 24 VLT "ferrobasalt" is richer in FeO than the Apollo 17 VLT basalt and is also highly feldspathic (12.5–14 weight percent Al_2O_3; Papike and Vaniman, 1978). In addition, the Luna 24 core contains an MgO-rich olivine basalt and, possibly, several additional types or subtypes (for example, see Ma and others, 1978). The spectra indicate the presence of additional units of Mare Crisium that were not sampled. Discovery of the VLT basalt caused a rethinking of previous classification schemes (Papike and Vaniman, 1978). In general, current thinking favors a continuum of lunar-basalt types rather than the pigeonhole classifications that emerged from earlier missions.

Despite the small sample size, accurate absolute ages of the underlying bedrock apparently were obtained from the regolith fragments (table 11.3; Lunatic Asylum, 1978). Identical Sm-Nd and ^{40}Ar-^{39}Ar ages fix the crystallization age of the Luna 24 VLT ferrobasalt at 3.30 aeons (Lunatic Asylum, 1978). The Lunatic Asylum (1978) did not regard Rb-Sr ages as reliable for these basalt samples, and so none are given here. An Ar-Ar age for a different sample that is 0.3 aeon older (table 11.1; Stettler and Albarede, 1978), and the presence of the buried Mg-rich basalt (Andre and others, 1978; Head and others, 1978a), suggest an extended history of basalt extrusion in Mare Crisium.

Summary and interpretation

The properties of Mare Crisium are consistent with excavation of a large, young, deep basin in a previously thick crust. I speculate that relatively thick crustal material favored aluminous mare volcanism and resistance to deformation, as in Mare Fecunditatis. Unlike Fecunditatis, however, the Crisium basin was filled by thick basalt because it had not been filled previously by thick basin ejecta (fig. 11.17). An older and smaller basin filled by thick earlier deposits would resemble Fecunditatis. A smaller basin of the same (Nectarian) age as Crisium would contain a small mare like Nectaris if it were in the same position as Crisium, or a large mare like Serenitatis if it were inside the Procellarum basin.

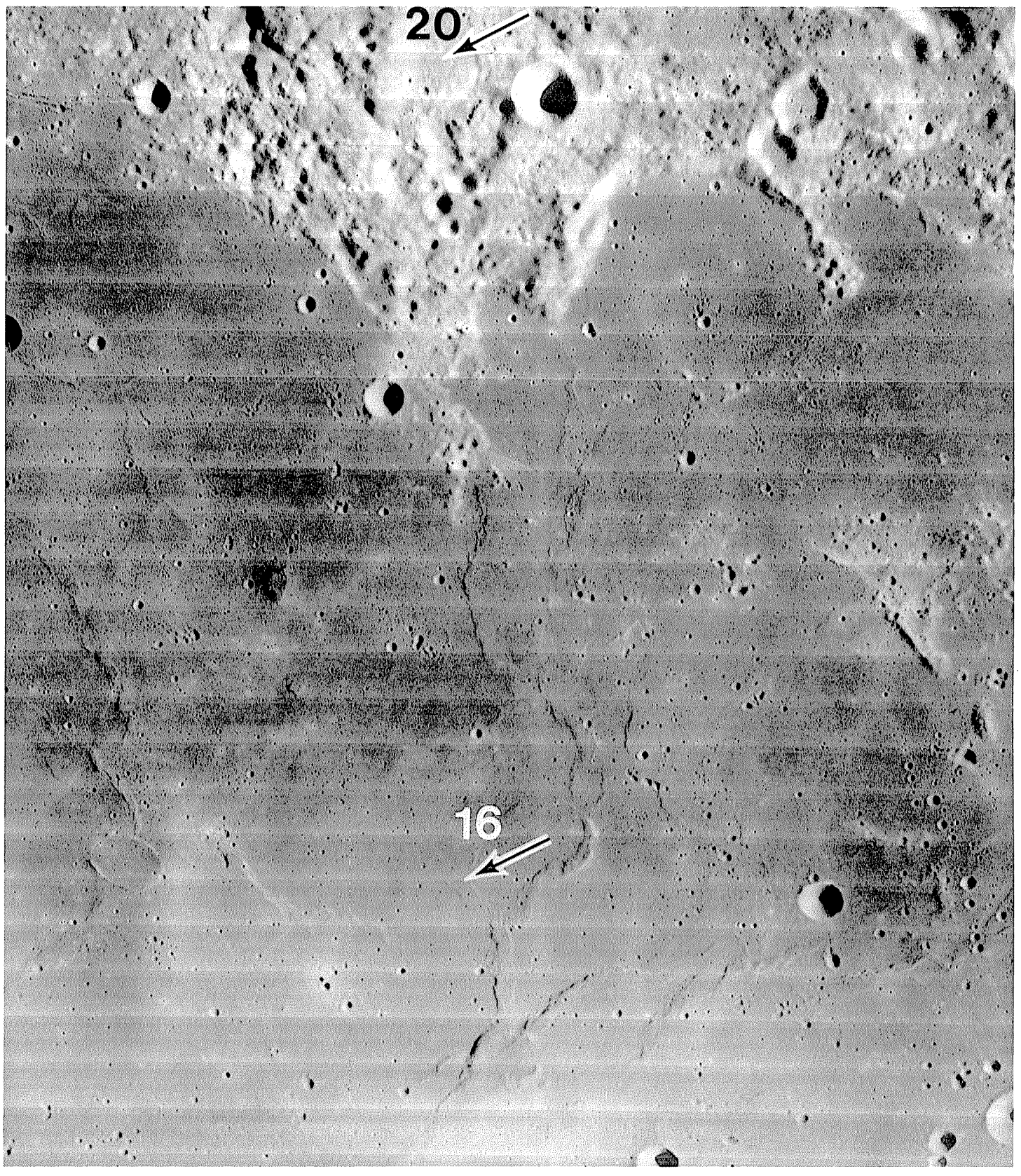

FIGURE 11.16.—Mare Fecunditatis and south Crisium-basin rim, showing Luna 16 and Luna 20 (see chap. 9) landing sites. Orbiter I frame M–33.

MARE IMBRIUM

General stratigraphy

The center of Mare Imbrium contains the Moon's thickest known mare-basalt section; the 1-km isopach extends to the largest diameter of all lunar maria and probably encloses several kilometers of basalt in the center (De Hon, 1979). Subsidence has opened large concentric grabens on the Apennine Bench and, in lesser degree, elsewhere (pl. 5; figs. 6.10, 10.7). Deformation was undoubtedly great in other, now-buried sectors, as is shown by Orientale, where most grabens would be buried if filled by a larger mare. Mare Imbrium has a large mascon, though not so large (table 6.1) as would be expected from the Moon's third largest basin (after Procellarum and South Pole-Aitken). The thin lithosphere may have allowed a more complete isostatic adjustment here than at Crisium.

The mare units of Imbrian age in Mare Imbrium are mostly spectrally red and bright (pl. 4; fig. 5.20; Head and others, 1978b). As in central Serenitatis, these units are more complex than can be shown in plate 9 and consist of a patchwork of units ranging in age from early to late Late Imbrian ($D_L = 240–385$ m; Boyce and others, 1975; Boyce, 1976; Wilhelms, 1980). Eratosthenian mare materials in Mare Imbrium are dark and relatively blue (see chap. 12). The spectrally red and blue types contrast sharply with each other but are each relatively uniform internally.

The Mare Frigoris-Sinus Roris trough is concentric with both the Imbrium and Procellarum basins (pls. 3, 4). It contains generally bright and thin mare materials of different spectral classes from most of Oceanus Procellarum but similar to some of the older units in the adjacent part of northern Mare Imbrium (pl. 4).

Apollo 15 samples—Palus Putredinis

Apollo 15, the first complex Apollo mission, was able to explore a wide area of both mare and terra systematically (see chap. 10). The peculiar sinuous rille Rima Hadley (figs. 5.11, 10.7, 10.9) helped attract attention to the landing site, which lies in the marginal mare of Mare Imbrium called Palus Putredinis. At one time, the rille or its source crater was thought to be a possible source of rare lunar volatile materials, although this hope faded with analyses of the volatile-free Apollo 11 basalt samples. The spectrally red mare of Palus Putredinis was a bonus to the more significant mission objective, materials of the Imbrium-basin rim (chap. 10; McCord and others, 1972b). This color indicates a low Ti content (Pieters, 1978), and the returned basalt samples contain much less of this element (1.5–2.0 weight percent TiO_2) than any other mare suite except that of Luna 24. The Palus Putredinis mare differs somewhat in remotely sensed properties from the spectrally red part of Mare Imbrium proper (Head and others, 1978b). Before the mission, the mare's age was correctly determined by the Trask method (see chap. 7; figs. 7.12–7.14) as near the Imbrian-Eratosthenian boundary (Carr and others, 1971). As was true for Apollo 17, more rock-size mare-basalt samples than terra materials were returned because the basalt was more accessible.

A twofold classification of the samples into an older, dominant type A and a younger, less abundant type B that was proposed upon preliminary examination of the field relations, modal mineralogy, and textures of the returned samples (Swann and others, 1972) has withstood further testing (for example, Rhodes and Hubbard, 1973; Lofgren and others, 1975). Type A is now generally referred to as quartz-normative or pigeonite basalt, and type B as olivine-normative or olivine basalt (table 5.2). Two conspicuous types of pyroclastic materials are also among the returned samples.

Pigeonite basalt.—The basalt type richer in silica is characterized by abundant modal pyroxene, mostly pigeonite with augite mantles. This basalt composes most of the rock-size samples collected by Apollo 15. It is exposed in boulders that are nearly in place at the rille lip (sta. 9A, fig. 10.9) and in ejecta of the major craters Elbow (400 m diam, max 80 m deep; sta. 1) and Dune (460 m diam, max 90 m deep; sta. 4). Textures are mostly porphyritic, and the groundmass of one subgroup is megascopically glassy (vitrophyric). The various textures are compatible with derivation from a single flow (Lofgren and others, 1975). Judging from the field relations, this flow constitutes most or all of the 60-m-thick section of layered lavas exposed in the walls of Hadley rille (figs. 1.10*B*, 11.18; Howard and others, 1972; Swann and others, 1972; Lofgren and others, 1975). The Apennine Bench Formation, which may be the source of small KREEP-rich fragments in the regolith (see chap. 10), may underlie this flow or a still older mare-basalt flow (fig. 11.18).

The best Ar-Ar ages of rocks and of smaller samples collected by a rake cluster between 3.30 and 3.32 aeons (table 11.3); Rb-Sr ages range from 3.21 to 3.37 aeons. Despite this spread in Rb-Sr ages, petrologic and chemical relations among the samples indicate moderate crystal fractionation of a single magma on or near the surface (Rhodes and Hubbard, 1973). The average crystallization age of the samples dated by both methods is 3.30 aeons.

Olivine basalt.—Rock-size olivine basalt was collected only from station 9A at the edge of Rima Hadley and from station 3 at Rhysling Crater (Swann and others, 1972). The near-surface position of the olivine basalt suggested by this distribution is corroborated by its greater abundance in smaller fragments, at all collection stations, than the pigeonite basalt (Swann and others, 1972; Rhodes and Hubbard, 1973; Lofgren and others, 1975). The petrologic and compositional data are consistent with derivation from a single flow different

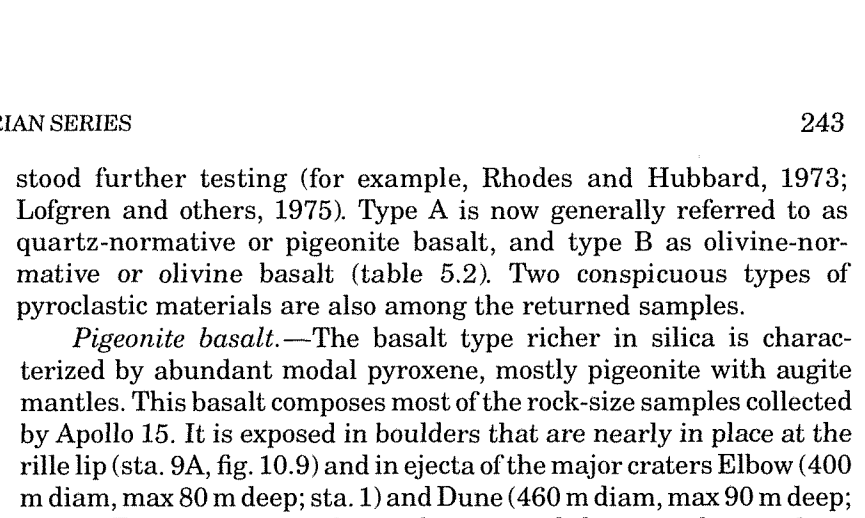

FIGURE 11.18.—Geologic cross section of mare materials at Apollo 15 landing site, drawn northwest-southeast on figure 10.7. Rima Hadley profile is from Howard and others (1972). Thicknesses of basalt units and presence of older basalt and Apennine Bench Formation are hypothetical.

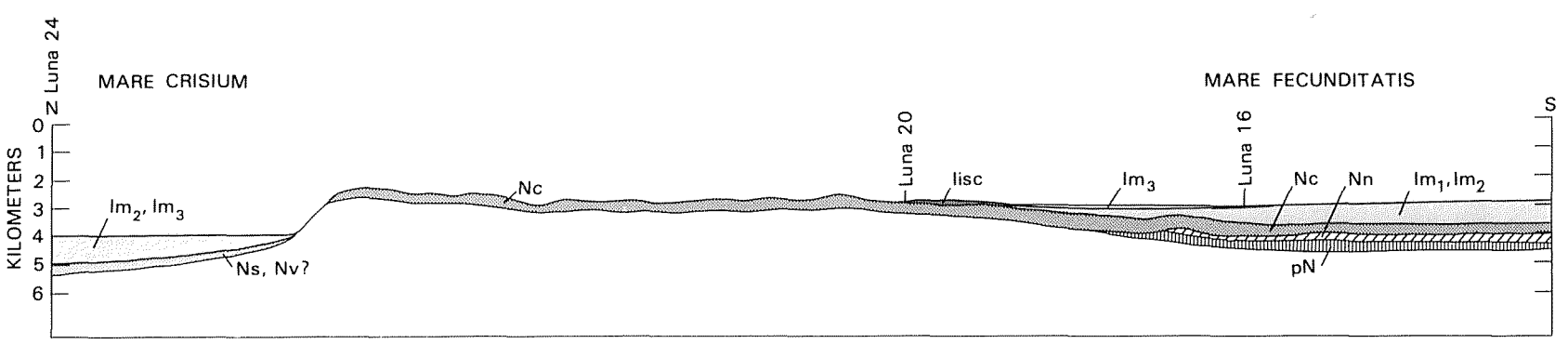

FIGURE 11.17.—Inferred geologic cross section in Crisium and Fecunditatis basins, drawn along line A'''–F in figure 8.4, with an extension to lat 5° S. Units, from oldest to youngest: pN, pre-Nectarian basin, crater, and volcanic deposits, undivided; Nn, Nectaris-basin ejecta; Nc, Crisium-basin ejecta (inner knobby and outer lineated types); Ns, Serenitatis-basin ejecta; Nv?, possible Nectarian volcanic deposits; Iisc, deposits of Imbrium-secondary craters; Im_1, Im_2, and Im_3, Imbrian mare units.

in parentage from the thicker pigeonite basalt flow (Rhodes and Hubbard, 1973).

The 9.6-kg porphyritic olivine-basalt boulder-size sample 15555 ("Great Scott") from station 9A has been dated by three geochronologic methods at 3.25 ± 0.05 aeons (table 11.3). One other rock (sample 15016) and numerous walnut-size rake samples from many collection stations average 3.27 aeons in age (Husain, 1974); the average by all methods is 3.26 aeons. This younger age is consistent with stratigraphic superposition on the pigeonite basalt but may not be significant in view of the spread in age determinations for each flow; the 40-million-year age difference between flows is just at the limit of geochronologic discriminability.

Pyroclastic green glass.—Apollo 15 also collected more pyroclastic material than did any other mission except Apollo 17. Green-glass droplets attracted the astronauts' attention and were collected from the regolith at two main stations (table 11.3). Emplacement by both impact and volcanism has been considered (see summary by Delano, 1979). Delano (1979) suggested that compositional data that were once seen as supporting evidence for an impact origin are more consistent with a volcanic origin. He proposed a derivation from heterogeneous sources rich in volatile material at 400 ± 50-km depth.

Although some older ages have been reported in the literature for the green glass, ages close to those of the lavas appear to be more likely (table 11.3). A dark-mantling deposit observed photogeologically near the landing site (Carr and others, 1971) could be the source of the green-glass samples (Carr and Meyer, 1974). However, the green glass, which is not dark in hand specimen, may be from a mantling deposit not detected either photogeologically or spectrally.

Pyroclastic red glass.—Droplets of red glass were also recovered by Apollo 15. Because this glass was found at only one station (6), it may be exotic to the landing site (Quaide, 1973). Delano (1980) suggested that its parent magma formed at the great depth of 480 km.

Summary and interpretation

Mare Imbrium is similar to western Mare Serenitatis in general stratigraphic sequence. Old, spectrally blue border basalt typical of eastern Serenitatis is not exposed. The main basin-filling sequence in both maria is thick, Ti-poor, relatively uniform spectrally, but complex in internal stratigraphy. Both sequences occasioned substantial basin subsidence, and both were followed by lesser amounts of spectrally blue Eratosthenian basalt erupted from the basin margins—more in Imbrium than in Serenitatis. These similarities probably result from superposition of the two relatively young basins on the thin lithosphere and crust in the central Procellarum basin (figs. 8.4, 11.14).

OTHER MARIA INSIDE THE PROCELLARUM BASIN

The outermost shelf of Oceanus Procellarum contains a large expanse of basalt of the youngest Late Imbrian age group (pl. 9). Most of this tract belongs to the same spectral class as central Serenitatis (mISP, pl. 4) but may be poorer in Fe (Basaltic Volcanism Study Project, 1981, p. 455). This young Late Imbrian basalt transects older Late Imbrian mare units and is overlain in places by Eratosthenian units (fig. 11.8). At the north end of the mare-filled part of the shelf and in the adjacent middle trough of the Procellarum basin, intermediate-age Upper Imbrian material of red spectral class LBG- overlaps the very old, spectrally blue units (class hDWA; Luna 16 type) perched on the mare margin. Class LBG- (unit 11, pl. 4) is also typical of Lacus Somniorum, in the eastern hemisphere, where intermediate-age and old Late Imbrian mare units overlie the same shelf and trough of the Procellarum basin (pls. 4, 9). Spectrally blue Eratosthenian units occupy the middle trough in much of the western nearside and locally extend onto the outer shelf (see chap. 12; pl. 10; fig. 12.11). The persistence of similar concentric compositional patterns in so much of the Procellarum basin, in otherwise different geologic settings, is remarkable.

The middle Procellarum trough is also the site of the Moon's three largest complexes of nonplanar volcanic deposits and unusual landforms (see chap. 5; pl. 4). The northernmost complex is the Rümker Hills (Mons Rümker), which consists of domes and dark-mantling deposits (fig. 5.9). Intermediate is the Aristarchus Plateau, which contains the Moon's largest and most numerous sinuous rilles and thick dark-mantling materials (fig. 5.12; Zisk and others, 1977). Farther south are the Marius Hills, characterized by diverse cones, domes, and sinuous rilles (fig. 5.7; McCauley, 1967a, 1968, 1969b). Although the morphologic freshness of the landforms in these three complexes suggests an Eratosthenian or even a Copernican age (Moore, 1965, 1967; McCauley, 1967a, b; Wilhelms and McCauley, 1971), they are partly flooded by late Late Imbrian lavas and so are mostly or entirely Imbrian in age (Zisk and others, 1977). The middle Procellarum trough apparently was conducive not only to late volcanism but also to extrusion of diverse magma types.

Oceanus Procellarum and other western-hemisphere maria east of long 40 W. have complex, mottled patterns of unit distribution that cannot be completely portrayed here (see Pieters and others, 1980; Whitford-Stark and Head, 1980; Wilhelms, 1980). Much of this region is covered by spectral class mIG- (Apollo 12 type), which represents a class of related compositional units (see chap. 5; Pieters, 1978). This complexity probably results from superposition on the larger Procellarum-basin structures of several old basins, such as Flamsteed-Billy, Insularum, Nubium (pl. 3), and the small basin or large crater that contains Mare Cognitum. The lithospheric and mantle structure resulting from these superpositions is complex and presumably influences a complex pattern of mare extrusion.

Oceanus Procellarum is generally stated to be a nonmascon mare, but, in fact, parts of its outer troughs contain small linear positive anomalies (Scott, 1974). Although Scott (1974) ascribed these anomalies to intrusion of dikes beneath linear mare ridges (fig. 6.2), I suggest that they are due to relatively thick sections of basalt in the troughs. They alternate with parallel negative anomalies aligned along the buried rings of the Procellarum basin (compare pl. 3 with fig. 2 of Scott, 1974).

The Procellarum pattern of mare distribution seems to persist into Mare Humorum, which has the third large mascon inside the Procellarum basin (besides Serenitatis and Imbrium; see table 6.1). Mare Humorum occupies the complex Nectarian Humorum basin (see chap. 9; figs. 4.3*U*, 9.24), which is superposed on the outer Procellarum shelf and periphery. The central mare is the most extensive, but maria are also abundant in parts of the north basin periphery that overlie the Procellarum basin (pl. 4). The presence of numerous conspicuous grabens (figs. 6.9, 9.24) indicates considerable subsidence. Mare Humorum contains mare units of diverse color (pl. 4) and age classes (Pieters and others, 1975; Boyce, 1976; Boyce and Johnson, 1978). The western part of the basin contains spectral class mISP, and the eastern part mIG-, as in Oceanus Procellarum. This relatively red unit is covered by a young (late Imbrian and (or) Eratosthenian), moderately blue unit originating outside central Mare Humorum. The southern contact between the mare and the basin is draped by a dark-mantling deposit called the Doppelmayer Formation (Titley, 1967).

The central highlands of the Moon apparently were a barrier to mare extrusion (pls. 4, 9; fig. 1.8). Between the Insularum-Nubium and Tranquillitatis-Asperitatis mare zones, hardly any maria occupy the zone between the Procellarum-basin rim and middle ring. Furthermore, the maria inside the middle ring are much smaller than elsewhere in the same radial position from the Procellarum center; they apparently required the additional lithospheric penetration afforded by such small basins or large craters as Vaporum, Aestuum (Wilhelms, 1968), and, possibly, a circular Sinus Medii structure (De Hon, 1979) not mapped here. The terra borders of these maria are rich in dark-mantling deposits (Wilhelms, 1968; Wilhelms and McCauley, 1971). Penetration by the Mutus-Vlacq and Werner-Airy basins was apparently insufficient to allow Late Imbrian volcanism, although pre-Nectarian basalt may be buried by ejecta plains in the Mutus-Vlacq basin (see chaps. 8, 9), and a small dark deposit in the crater Airy may be volcanic in origin (unless it is ejected Imbrium-basin impact melt). Thus, the south-central terra "backbone" may be a first-order crustal feature. A northward extension seems to block mare extrusion in the central part of the outer Procellarum trough (pl. 4). These major terra structures may have arisen during the "magma ocean" stage, or they may be remnants spared from excavation by giant undiscovered basins still older than Procellarum.

NEAR-LIMB MARIA OUTSIDE THE PROCELLARUM BASIN

Mare Orientale and Mare Smythii are similar in many respects. They are thin mascon maria (Solomon and Head, 1980), and their basins are of about the same size (table 4.1). They also are equally deep (Sjogren and Wollenhaupt, 1976; Strain and El-Baz, 1979)—a surprising fact at first glance, considering the difference in age of their basins (Imbrian and pre-Nectarian, respectively). Both basins contain floor-rebound craters (pl. 5); Smythii has more because it is the older basin and thus contains more craters of all types. The ring-and-trough structure is similar in the two basins (Strain and El-Baz, 1979). Smythii lacks arcuate grabens, and those of Orientale, though conspicuous and numerous, are confined to a smaller area of the basin than those in more deeply filled maria (pl. 5; table 6.1). The paucity of grabens is expected from their position on a thick lithosphere, which resisted vertical movements in both basins.

As in other maria superposed on thick terra crusts, the Smythii basalt appears to be highly aluminous (Conca and Hubbard, 1979; Hubbard, 1979), although this appearance may result from mixing of the thin mare with terra material (P.D. Spudis, oral commun., 1982). Like Crisium, Smythii is low in radioactivity (Metzger and others, 1977). Mare Orientale was not analyzed.

The two maria apparently had somewhat different patterns of basalt emplacement. Smythii contains late Imbrian units (pl. 9) thinly covered by Eratosthenian units (pl. 10; Boyce and Johnson, 1978). At Orientale, extrusion ended during the middle Late Imbrian in the central mare, which is comparable to all of Mare Smythii, but migrated to the inner and then to the outer crescentic maria in the concentric troughs (Lacus Veris and Autumni, respectively; Greeley, 1976).

Small, thin, old maria occupy some of the terrain between the Humboldtianum and Procellarum basins in the northeast quadrant of the nearside (pl. 9; fig. 9.3). A very old, still-undelineated basin may exist in this region.

Mare Australe probably contains a more nearly equal amount of all three Imbrian mare units than any other studied mare (pl. 9). Most of the maria occupy craters superposed on the Australe basin, and much less basalt probably would have erupted in this shallow weakly defined basin if these craters were absent. Mare ridges, but not grabens, are present (pl. 5; Wilhelms and others, 1979).

Mare Marginis is another near-limb mare that contains old (fig. 4.7) as well as young (Boyce and Johnson, 1978) mare units. Some of the basalt is KREEP-rich (Hawke and Spudis, 1980).

FARSIDE MARIA

Most maria that lie entirely on the farside are poorly characterized because of absence of telescopic spectra, paucity of orbital geochemical readings, and poor photographic coverage (pl. 2). No arcuate grabens are known, and they are probably absent (pl. 5). I know of only five farside mare patches that have been dated by crater counts (Wilbur, 1978; Walker and El-Baz, 1982), all of which indicate a middle Late Imbrian age (pl. 9).

The farside's most extensive maria, those in the South Pole-Aitken basin, are similar to those of Australe in that they occupy parts of small superposed basins (pls. 4, 9) and large craters. Thus, South Pole-Aitken played a lithosphere-thinning role on the farside comparable to that of the Procellarum basin on the nearside. The fact that maria are sparser in South Pole-Aitken than in Procellarum is probably due to: (1) the smaller size of South Pole-Aitken, 2,500 versus 3,200 km; (2) the absence of such large superposed basins as Imbrium and Serenitatis; and, possibly, (3) a first-order hemispheric dichotomy in crustal thickness, such as is commonly hypothesized (see chaps. 1, 6, 8).

Other farside maria are scattered in the few other large basins, in a few large craters, or in such seemingly isolated and unexplained spots as the crater Kohlschütter and Lacus Solitudinis (pl. 4; figs. 5.2, 5.3). The Moscoviense basin contains the largest mare patch outside the South Pole-Aitken basin; photographic coverage is inadequate for dating the mare, but it appears to be old. The mare's relatively large area may result from superposition of two basins (D.E. Davis, oral commun., 1982), only one of which is mapped here. The conspicuous mare in crater Tsiolkovskiy probably results from the considerable depth of this large Late Imbrian crater, aided by its superposition on the Tsiolkovskiy-Stark basin. The mare, which is covered by one of the best Lunar Orbiter photographs of the farside (an Orbiter 3 H-frame; pl. 2), is Imbrian in age. D_L values of 255 m (Boyce and others, 1975) suggest a late Late Imbrian age, whereas crater frequencies (Wilbur, 1978; Walker and El-Baz, 1982) suggest a middle Late Imbrian age. The basalt may be rich in Ti (Metzger and others, 1977; Wilbur, 1978). Finally, pre-Imbrian or Early Imbrian basaltic plains are likely to be hidden beneath the smooth, light-colored plains fillings of such basins as Hertzsprung and Korolev (see chap. 9).

CHRONOLOGY

Late Imbrian mare basalt is the most accurately dated lunar material. The Late Imbrian Epoch began immediately after the Orientale impact, which is estimated from superposed crater frequencies to have occurred 3.8 aeons ago, between the Imbrium impact 3.85 aeons ago and the extrusion of the Apollo 17 mare basalt 3.72 aeons ago (see chap. 10). The youngest sampled Imbrian mare basalt, from the Apollo 15 landing site, formed 3.26 aeons ago. Therefore, the Late Imbrian Epoch lasted at least 0.54 aeon and probably a little longer, allowing for extrusion of some unsampled units after 3.26 aeons (for example, in Maria Serenitatis and Crisium; table 11.1). An approximate date of 3.2 aeons ago, between the Apollo 15 and Apollo 12 dates, is adopted here for the end of the Late Imbrian Epoch and the Imbrian Period. Therefore, the Late Imbrian Epoch lasted about 0.60 aeons and the Imbrian Period about 0.65 aeons.

Exposed basalt units of the oldest of the three Late Imbrian age groups mapped here are all on the outer shelf of the Procellarum basin or outside that basin. Their age is estimated at from 3.75 to 3.80 aeons; the exposed flows were not sampled, but the 3.79-aeon Ar-Ar age of one sample from a buried unit at the Apollo 11 landing site (10062; table 11.1) lies within this age range.

Exposed flows of the intermediate-age group are represented by the Apollo 17 Ti-rich basalt (3.72 aeons) and the Apollo 11 high-K, Ti-rich basalt (3.57 aeons). The age range of this group suggested by these absolute ages, as calibrated with the relative stratigraphy, is 3.50 to 3.75 aeons. In addition, therefore, an Apollo 16 fragment probably from Mare Nectaris (3.74 aeons), two low-K, high-Ti Apollo 11 units (3.67 and 3.70 aeons), and the Apollo 17 pyroclastic deposit (3.64 aeons) also probably originated in middle Late Imbrian time. Orbital geochemistry indicates that compositions of this age are very diverse. Many units are deformed by grabens.

The youngest Late Imbrian age group, 3.20 to 3.50 aeons old, is represented by the Luna 16 feldspathic basalt (3.40 aeons), the Luna 24 VLT basalt (3.30 aeons), the Apollo 15 green glass (3.30 aeons), and the Apollo 15 low-Ti olivine basalt and pigeonite basalt (3.26 and 3.30 aeons, respectively). Few units of this group are cut by grabens, but most are deformed by mare ridges. Spectrally red or "orange" basalt units with medium to low Ti contents characterize the most extensive exposures of this age group, that is, those in Mare Serenitatis, Mare Imbrium, and western Oceanus Procellarum. Basalt of this composition may be the Moon's most voluminous basaltic type.

Dark-mantling materials lie at the margins of most maria but predominate around maria superposed on the center and intermediate trough of the Procellarum basin. Many of these dark-mantling deposits are older than the adjacent lavas. Spewing of magmas driven by volatile materials probably was important in the early filling of basins (Head, 1974a). At 3.64 aeons, the middle Late Imbrian Apollo 17 orange and black glass is somewhat younger than the subjacent Apollo 17 lavas (3.72 aeons). The 3.3-aeon age of the Apollo 15 green glass shows that pyroclastic materials were also erupted late in the Late Imbrian Epoch.

In the Imbrian Period, the cratering rate changed from the intensive early bombardment (fig. 8.16) to a much-reduced rate that characterizes the rest of lunar history. This rapid falloff in impact rate is recorded by successively lower crater densities for successively younger time-stratigraphic units (pls. 7–11; figs. 7.16, 8.6, 9.22, 10.4). During the total Imbrian Period, 9.7 craters larger than 30 km in diameter formed per million square kilometers (pls. 8, 9), in contrast to about 35 such craters in the Nectarian Period and more than 77 in pre-Nectarian time. If the Orientale basin formed 3.8 aeons ago and the Late Imbrian Epoch ended 3.2 aeons ago, formation of the 195 Lower Imbrian craters of this size on the whole Moon required 0.05 aeons, and that of the 174 Upper Imbrian craters required 0.6 aeons.

These values translate into rates of 3,900 and 290 impacts per aeon, respectively. These rates are transitional between the 19,000 impacts per aeon of the Nectarian Period (1,330 craters in 0.07 aeon) and the much lower Eratosthenian and Copernican rates of 42 impacts per aeon (133 craters in 3.2 aeons). Errors in the durations of the periods and epochs proposed here would change these values but would not alter the conclusion that the rate of impacts decreased sharply between 3.85 and 3.2 aeons ago.